DEVELOPMENTS OF THE INTRINSIC LOW DIMENSIONAL MANIFOLD METHOD AND APPLICATION OF THE METHOD TO A MODEL OF THE GLUCOSE REGULATORY SYSTEM

A Thesis

Submitted to the Graduate School
of the University of Notre Dame
in Partial Fulfillment of the Requirements
for the Degree of

Master of Science in Mechanical Engineering

by

Rafael E. Petrosyan, Master of Science in Applied Mathematics and Physics

---

Dr. Joseph M. Powers, Director

Department of Aerospace and Mechanical Engineering
Notre Dame, Indiana
April 2003

DEVELOPMENTS OF THE INTRINSIC LOW DIMENSIONAL MANIFOLD METHOD AND APPLICATION OF THE METHOD TO A MODEL OF THE GLUCOSE REGULATORY SYSTEM

Abstract

by

Rafael E. Petrosyan

This thesis addresses two major topics: theoretical and numerical development of the Intrinsic Low Dimensional Manifold (ILDM) Method for systems of Ordinary Differential Equations (ODEs) and application of ILDM method to the analysis of the glucose regulatory system. A large spectral gap in the eigenvalue spectrum is found to provide a sufficient condition of the applicability of the ILDM method in a small neighborhood of the equilibrium point. A simple adaptive parameterization technique is developed to implement the ILDM method numerically. The ILDM method is used to analyze a coupled glucose-insulin-β-cells model of the glucose regulatory system. The ILDM models well the late-time dynamics of the system. Through stability analysis the pathways to diabetes were formally verified.

CONTENTS

TABLES

FIGURES

ACKNOWLEDGEMENTS

I would like to acknowledge my advisor, Dr. Joseph M. Powers, for his guidance throughout my graduate studies. Furthermore, I would like to acknowledge Dr. Alex Himonas and Dr. Samuel Paolucci for taking the time to be on my masters committee. I also would like to acknowledge Ms. Sue E. Kostry for her help with the editorial work on the thesis.

CHAPTER 1

INTRODUCTION

1.1 Overview

The primary motivation for the current work is to demonstrate usefulness of the ILDM method in analysis of the dynamical systems which arise in biology. The method was introduced in 1992 by Maas and Pope [15] as a dimension reduction technique for stiff chemically reactive systems. A chemically reactive system is called stiff if the ratio of the most negative eigenvalue to the least negative eigenvalue is a large number. The method uses the fact that provided the difference in time scales is large, a system, once fast processes are equilibrated, comes to the slow manifold of a dimension lower than that of the original system and stays on that manifold all the way down to the equilibrium point. *A priori* equilibration of the fast processes allows one not only to reduce the dimension of a problem, but more importantly to considerably reduce the computational time, because it is the fast processes that require small time steps. The technique uses local equilibration that gives better accuracy compared with classical approaches such as the steady state approximation [7]. These features made the ILDM method a useful tool for solving large and stiff systems of nonlinear differential equations which arise in combustion problems. The method provides an algorithm for *a priori* computation of the slow low dimensional manifolds. The algorithm consists of solving an algebraic system of equations in a subspace of the full phase space. Finding the slow manifold is important for understanding of the global behavior of a stiff dynamical system,

because, no matter what the initial conditions are, such a system evolves on the manifold for most of the time. Since dynamical systems in biology often result from the application of a mass action law and have stable sink type equilibrium points, the situation similar to Arrenius kinetics, it seems natural to apply the method to that type of biological problems. At this point, using the method to understand the global behavior of the dynamical systems in biology seems to be a primary application, because modeling of the biological processes is still in the developmental stage for most of the problems, however, with time, as more complicated and detailed models will appear, the ILDM method promises to become useful as a tool for practical solution of the systems of ordinary differential equations in that field.

A large part of the current thesis concerns theoretical development of the ILDM method from the point of mathematical justification. The motivation for this part of the study is the fact that despite a rather large number of works on the ILDM method, there is a lack of theoretical studies involving a rigorous derivation of the formulas constituting the technique. To the knowledge of the author, the only work done in that direction up to this time is that of Wiggins and co-workers [19]. In the current work, the ILDM theory for an arbitrary nonlinear system with a stable sink type point is built based upon the only assumption of a large gap in the eigenvalue spectrum computed at the equilibrium point. It is shown that if the quantity inverse to the spectral gap is used as a small parameter, the Maas-Pope formula is derived as a first approximation to the solution of the resulting singular perturbation problem. The result proved provides a sufficient condition for the applicability of the ILDM approximation in a small neighborhood of the equilibrium point and gives the order(s) of the ILDM(s) that correctly approximate the solution of the original system. This development represents an important result of the current work.

The Maas-Pope formula defines the ILDM locally and hence needs to be linked with a continuation algorithm. In their original paper [15], Maas and Pope offered to use a rather complicated arc length continuation method (see for example [8]). Here, we develop an alternative technique, which has the advantage of a simple programming realization in the case of a one-dimensional ILDM. This represents the second result of the current work.

To demonstrate the ILDM method, we analyze a coupled glucose-insulin-β-cells model of the glucose regulatory system. The model, introduced by Topp, *et al.* [24], was chosen, because it has all its three time scales separated, and hence both one- and two-dimensional ILDMs can be used to approximate the solution. The main result here is that the two-dimensional manifold obtained with the use of the ILDM method provided better understanding of the dynamics compared to classical approaches used by the authors of the original paper [24].

1.2 The Intrinsic Low Dimensional Manifold (ILDM) method

The ILDM method is a technique of finding an approximation of the slow manifold(s) of a stiff system of nonlinear ODEs and using the manifold(s) to obtain an approximate solution of that system. The approximation of the slow manifold obtained with the method is also called the ILDM.

The slow manifold can be roughly defined as the subset of the phase space that all the solutions of the system come to and stay on after fast time scale events are equilibrated. This definition implies that the slow manifold must be a solution itself (in the case of a first order manifold) or be formed by a continuum set of solutions (in the case of the manifolds of higher order). This immediately follows from the fact that if we chose initial conditions to be on the slow manifold, the solution should stay on it all the way to the equilibrium point. This simple fact can be used to obtain a functional equation for the slow manifold. This equation was obtained by

Fraser [12] and studied by Roussel and Fraser [20] and Davis and Skodje [7]. It was solved in a few simple cases, however poor convergence properties make this approach difficult to use for solving real problems.

Maas and Pope [15] introduced an approximate formula for computing the slow manifold. They called the technique the ILDM method, the approximation was called the ILDM as well. The formula locally defines the slow manifold through the fast part of the inverse eigenvector matrix. The method proved to be useful for solving real problems; however, no proof of the formula was offered. In this work, we build the theory upon the only assumption of a gap in the eigenvalue spectrum at the equilibrium point. We prove the Maas-Pope formula and give a sufficient condition of using the ILDM of an arbitrary order to approximate the solution of the original system.

Since the time the technique was introduced, a rather large number of works, concerning developments and applications of the Maas-Pope algorithm, have been published. (see for example [25], [17], [21]). Finally, we would like to mention that attempts have been made to extend the method to reaction-diffusion equations [22].

1.3 Glucose regulatory system

Blood glucose levels are regulated by two negative feedback loops. In the short term hyperglycemia stimulates a rapid increase in insulin release from the pancreatic β cells. The associated increase in blood insulin levels causes increased glucose uptake and decreased glucose production leading to a reduction in blood glucose [2]. Chronic hyperglycemia may contribute to a second negative feedback loop by increasing the mass of insulin secreting β cells, through changes in β cells' replication [13] and death [9] rates. An increased β cell mass represents an increased capacity for insulin secretion which, in turn, would lead to a decrease in blood glucose.

Diabetes mellitus is a disease of the glucose regulatory system characterized by

fasting and/or postprandial hyperglycemia. There are two types of diabetes. Type 1 diabetes (insulin dependent diabetes) is due to autoimmune attack on the insulin secreting β-cells. It is accompanied by 80-90 % loss in β-cell mass [14]. Type 2 diabetes (noninsulin dependent diabetes) is associated with a deficit in the mass of β cells, reduced insulin secretion and resistance to the action of insulin. It is accompanied by 40-50 % loss of β-cell mass when compared with weight-matched non-diabetic subjects [14]. The experimental data suggests that multiple defects are required for onset of type 2 diabetes (see for example the discussion in [24]).

Mathematical modeling of diabetes has focused predominantly on the dynamics of a single variable, usually glucose or insulin level [3], [23]. Those models were usually used for measuring either rates (glucose, insulin production/uptake) or sensitivities (insulin sensitivity, glucose effectiveness). There were also studies that analyzed coupled glucose-insulin dynamics. In the current work we consider a first model that incorporates β-cell mass dynamics. This model was introduced by Topp, *et al.* [24]. The model uses a simple experimentally based formula for β-cell dynamics and correctly describes some of the experimentally established effects.

1.4 Thesis outline

The current thesis consists of four chapters. The introductory chapter contains a brief description of the work done and gives a brief description of the ILDM method and the biological problem considered in the thesis.

The ILDM method is considered in detail in the second chapter of the thesis. The ILDM theory is built consequently for three cases: linear systems, nonlinear systems with a single spectral gap and, finally, for nonlinear systems with an arbitrary number of spectral gaps. The rest of the chapter concerns the development of the adaptive parameterization technique for computing the slow manifolds of the first and the second orders.

In the third chapter, the ILDM method is used to analyze a coupled glucose-insulin-β-cells model of the glucose regulatory system. The chapter starts from the description of the model introduced by Topp, *et al.* [24]. Further, the results for one- and two-dimensional manifolds obtained with the use of the algorithm, considered in the second chapter, are presented, and a discussion of the results predicted by the model is given. Finally, stability analysis is performed, and the defects in the functioning of the glucose regulatory system that result in diabetes mellitus disease are considered.

The last chapter contains a brief discussion of the results and outlines possible directions for future research.

CHAPTER 2

THE ILDM METHOD

2.1 Theoretical basis of the ILDM method for a system of Ordinary Differential Equations (ODEs)

Let us consider an autonomous system of ODEs:

$$\frac{d\mathbf{y}}{dt} = \mathbf{f}(\mathbf{y}), \qquad \mathbf{y}(0) = \mathbf{y}_0, \qquad \mathbf{y} \in \mathbb{R}^n \tag{2.1}$$

Such systems can result from the law of mass action and model many processes studied in chemistry and biology. Physically, $\mathbf{y}$ usually represents concentrations of the elements, n represents the number of elements, t represents time, and $\mathbf{f}(\mathbf{y})$ is the source term which gives the rates of change of those concentrations due to interactions and other processes constituting a model. In many real situations these processes occur at widely different time scales. Such a difference induces stiffness into the system (2.1) and makes it computationally expensive to solve. We suppose that the system (2.1) has a stable sink type equilibrium point; that is, all the eigenvalues are distinct, real, and negative. Without loss of generality the equilibrium point can be transferred to the origin by a linear transformation. In general, the system (2.1) may have any number of sink type equilibrium points, but for the sake of simplicity, we restrict our consideration to systems which have only one such point, which is the case in many practical applications. It should be noted, however, that the analysis can be extended to the systems with an arbitrary number of sink type equilibrium points, with the difference, that the basins of attraction of all such points must be considered separately.

2.1.1 Linear systems

The idea of the method can be demonstrated on the example of a linear system. In the linear case we have:

$$\frac{d\mathbf{y}}{dt} = \mathbf{J}\mathbf{y}, \tag{2.2}$$

where $\mathbf{J} = \partial\mathbf{f}/\partial\mathbf{y}$ is a constant Jacobian matrix. The Jordan decomposition of the matrix is given by:

$$\mathbf{J} = \mathbf{V}\mathbf{\Lambda}\widetilde{\mathbf{V}}, \qquad \widetilde{\mathbf{V}} \equiv \mathbf{V}^{-1} \tag{2.3}$$

$$\mathbf{V} = \left(\begin{array}{ccc|ccc} | & & | & | & & | \\ \mathbf{v}_1 & \cdots & \mathbf{v}_m & \mathbf{v}_{m+1} & \cdots & \mathbf{v}_n \\ | & & | & | & & | \end{array}\right) = \left(\begin{array}{c|c} \mathbf{V}_s & \mathbf{V}_f \end{array}\right) \tag{2.4}$$

$$\mathbf{\Lambda} = \left(\begin{array}{ccc|ccc} \lambda_{(1)} & & 0 & & & \\ & \ddots & & & \mathbf{0} & \\ 0 & & \lambda_{(m)} & & & \\ \hline & & & \lambda_{(m+1)} & & 0 \\ & \mathbf{0} & & & \ddots & \\ & & & 0 & & \lambda_{(n)} \end{array}\right) = \left(\begin{array}{c|c} \mathbf{\Lambda}_{(s)} & \mathbf{0} \\ \hline \mathbf{0} & \mathbf{\Lambda}_{(f)} \end{array}\right) \tag{2.5}$$

$$\widetilde{\mathbf{V}} = \left(\begin{array}{ccc} - & \widetilde{\mathbf{v}}_1 & - \\ & \vdots & \\ - & \widetilde{\mathbf{v}}_m & - \\ \hline - & \widetilde{\mathbf{v}}_{m+1} & - \\ & \vdots & \\ - & \widetilde{\mathbf{v}}_n & - \end{array}\right) = \left(\begin{array}{c} \widetilde{\mathbf{V}}_s \\ \hline \widetilde{\mathbf{V}}_f \end{array}\right) \tag{2.6}$$

The notation in the equations above is taken from [22]. Here, $\mathbf{V}$ is the right eigenvector matrix, which contains the right eigenvectors of $\mathbf{J}$, $\mathbf{v}_1,\ldots,\mathbf{v}_n$ in its columns; $\mathbf{\Lambda}$ is the diagonal matrix, which contains eigenvalues $\lambda_{(1)},\ldots,\lambda_{(n)}$ of $\mathbf{J}$ along its main

diagonal, and $\widetilde{\mathbf{V}}$ is the inverse right eigenvector matrix, with rows formed by the $\widetilde{\mathbf{v}}_1,\ldots,\ \widetilde{\mathbf{v}}_n$, reciprocal to the right eigenvectors. It is important for the following discussion that the eigenvalues are ordered from the least negative to the most negative. Multiplying both sides of (2.2) on $\widetilde{\mathbf{V}}$ from the left and defining a new set of variables by $\mathbf{z} = \widetilde{\mathbf{V}}\mathbf{y}$ we obtain:

$$\frac{d\mathbf{z}}{dt} = \mathbf{\Lambda}\mathbf{z}, \tag{2.7}$$

which, in the Einstein notation, can be rewritten in the following form:

$$\frac{1}{\lambda_{(i)}}\frac{dz_i}{dt} = z_i, \qquad i = 1,\ldots,n. \tag{2.8}$$

The system (2.8) has a simple analytical solution; however, numerical integration even in such a simple case may be quite time consuming when the stiffness is high. A general way of handling stiff systems, which should be employed when the eigenvalues are located close to each other, consists in the using of an implicit difference scheme; however, if the eigenvalue's spectrum has a significant gap, then a more efficient technique can used. Without loss of generality, let us suppose, that there is a spectral gap between $|\lambda_{(m)}|$ and $|\lambda_{(m+1)}|$, that is $\varepsilon = |\lambda_{(m)}|/|\lambda_{(m+1)}| \ll 1$. Further, we rescale the time variable by $\tau = t|\lambda_{(m)}|$. It will be seen from what follows that the scaling factor corresponds to the fastest time scale to be resolved. Now, recalling that all the eigenvalues are negative numbers, one can rewrite the system (2.8) as follows:

$$\begin{aligned}
\frac{|\lambda_{(m)}|}{|\lambda_{(1)}|}\frac{dz_1}{d\tau} &= -z_1 \\
&\vdots \\
\frac{|\lambda_{(m)}|}{|\lambda_{(m-1)}|}\frac{dz_{m-1}}{d\tau} &= -z_{m-1} \\
\frac{dz_m}{d\tau} &= -z_m \\
\varepsilon\frac{dz_{m+1}}{d\tau} &= -z_{m+1}
\end{aligned} \tag{2.9}$$

$$
\begin{aligned}
\varepsilon \frac{dz_{m+2}}{d\tau} &= -\frac{|\lambda_{(m+2)}|}{|\lambda_{(m+1)}|} z_{m+2} \\
&\vdots \\
\varepsilon \frac{dz_n}{d\tau} &= -\frac{|\lambda_{(n)}|}{|\lambda_{(m+1)}|} z_n
\end{aligned}
$$

The system (2.9) constitutes a singular perturbation problem, with $\varepsilon = |\lambda_{(m)}|/|\lambda_{(m+1)}| \ll 1$ as a small parameter. For $\tau \gtrsim 1$, the dynamics of the system (2.9) can be approximated by neglecting the terms which are of the order of ε, and hence, for $\tau \gtrsim 1$, the system (2.9) can be approximated by:

$$
\begin{aligned}
\frac{|\lambda_{(m)}|}{|\lambda_{(1)}|} \frac{dz_1}{d\tau} &= -z_1 \\
&\vdots \\
\frac{|\lambda_{(m)}|}{|\lambda_{(m-1)}|} \frac{dz_{m-1}}{d\tau} &= -z_{m-1} \\
\frac{dz_m}{d\tau} &= -z_m \\
z_{m+1} &= 0 \\
&\vdots \\
z_n &= 0
\end{aligned}
\tag{2.10}
$$

The differential algebraic system (2.10) has reduced stiffness and the lesser number of differential equations compared to the original system. Geometrically, the system (2.10) evolves on an m-dimensional manifold instead of $\mathbb{R}^n$ and, therefore, the dimension of the problem has been reduced from n to m. A solution of the original system started at any point of the phase space comes down to the manifold during a time interval $\triangle\tau \lesssim 1$ or in terms of the original time variable $\triangle t \lesssim 1/|\lambda_{(m)}|$ and stays on it all the way down to the equilibrium point. The manifold is defined by the last $(n-m)$ equations of the system (2.10)

$$
z_i = 0, \qquad i = m+1, \ldots, n \tag{2.11}
$$

and is referred to as the ILDM. The technique, which involves solution of the reduced system (2.10) instead of the original system, is referred to as the ILDM method. It should be emphasized that the method approximates the dynamics of the original problem for $t \gtrsim 1/|\lambda_{(m)}|$ only, and hence, if one is interested in the dynamics for $t \lesssim 1/|\lambda_{(m)}|$ then the reduction must be done by rescaling the time variable $\tilde{\tau} = \tau|\lambda_{(n)}|/|\lambda_{(m)}|$ and taking the limit $|\lambda_{(m)}|/|\lambda_{(m+1)}| \to 0$ or alternatively the full system can be considered. Since the exact solution is known, one can estimate the error, which comes from the approximation of the original system with the reduced system (2.10). The error of approximating z_i by the system (2.10) is given by:

$$E_i = \begin{cases} 0 & i = 1, \ldots, m \\ z_{0_i} e^{-\frac{|\lambda_{(i)}|}{|\lambda_{(m+1)}|}\frac{\tau}{\varepsilon}} & i = m+1, \ldots, n, \end{cases} \tag{2.12}$$

where z_{0_i} are the initial values of corresponding z_i. Therefore, the maximum error coming from the approximation is given by

$$E_{(m+1)} = z_{0_{(m+1)}} e^{-\frac{\tau}{\varepsilon}} \tag{2.13}$$

and exponentially goes to 0 as the spectral gap increases. The other error associated with the method is the error of approximation of the slow manifold (SM) by the ILDM:

$$E_{SM} = SM - ILDM \tag{2.14}$$

Direct substitution shows that the ILDM (2.11) represents a solution of the original system (in the case of $m = 1$) and consists of a continuum number of the solutions (in the case of $m > 1$). Moreover, at every point of those solutions the fast time scales are equilibrated, and hence the ILDM coincides with the slow manifold. In this sense, the ILDM method is said to be exact for the linear systems.

2.1.2 Nonlinear systems with the only spectral gap

In the general case of nonlinear $\mathbf{f}(\mathbf{y})$, one can formally make use of a similar procedure. First, we define a new function $\mathbf{g}(\mathbf{y})$:

$$\mathbf{g} = \mathbf{f} - \mathbf{J}(\mathbf{y})\mathbf{y}, \tag{2.15}$$

and hence, the system (2.1) can be rewritten as follows:

$$\frac{d\mathbf{y}}{dt} = \mathbf{J}(\mathbf{y})\mathbf{y} + \mathbf{g}. \tag{2.16}$$

Further, we perform the symbolic Jordan decomposition $\mathbf{J} = \mathbf{V}\mathbf{\Lambda}\widetilde{\mathbf{V}}$ and as in the linear case define a new set of variables $\mathbf{z} = \widetilde{\mathbf{V}}\mathbf{y}$, so that the system (2.16) can be rewritten in the following way:

$$\frac{d\mathbf{z}}{dt} + \widetilde{\mathbf{V}}\frac{d\mathbf{V}}{dt}\mathbf{z} = \mathbf{\Lambda}\mathbf{z} + \widetilde{\mathbf{V}}\mathbf{g}, \tag{2.17}$$

or, equivalently, in the Einstein notation:

$$\frac{1}{\lambda_{(i)}}\left(\frac{dz_i}{dt} + \widetilde{\mathbf{v}}_i \sum_{j=1}^{n} \frac{d\mathbf{v}_j}{dt} z_j\right) = z_i + \frac{1}{\lambda_{(i)}}(\widetilde{\mathbf{v}}_i \mathbf{g}), \qquad i = 1, \ldots, n. \tag{2.18}$$

Equation 2.18 was also used in [22]. Compared to the linear case, the system (2.18) has two extra terms caused by nonlinearity. Moreover, the eigenvalues are no longer constants, but instead are functions defined on the phase space. However, sufficiently close to the equilibrium point analysis similar to that of in the linear case can be performed. First of all, we rescale $\lambda_{(i)}$, $i = 1, \ldots, n$, using the eigenvalues at the equilibrium as scaling factors, that is:

$$\lambda_{(i)} = -|\lambda_{(i)_0}|\widetilde{\lambda}_{(i)}, \qquad i = 1, \ldots, n, \tag{2.19}$$

where $\widetilde{\lambda}_{(i)}$ are positive functions of the order of 1. Further, like in the linear case, supposing that there exists a spectral gap between $|\lambda_{(m)_0}|$ and $|\lambda_{(m+1)_0}|$, so that

$\varepsilon = |\lambda_{(m)_0}|/|\lambda_{(m+1)_0}| \ll 1$, we rescale the time variable $\tau = t|\lambda_{(m)_0}|$, and rewrite (2.18) as follows:

$$\begin{aligned}
\frac{|\lambda_{(m)_0}|}{|\lambda_{(1)_0}|}\left(\frac{dz_1}{d\tau} + \widetilde{\mathbf{v}}_1 \sum_{j=1}^{n} \frac{d\mathbf{v}_j}{d\tau} z_j\right) &= -\widetilde{\lambda}_{(1)} z_1 + \frac{1}{|\lambda_{(1)_0}|}(\widetilde{\mathbf{v}}_1 \mathbf{g}), \\
&\vdots \\
\frac{|\lambda_{(m)_0}|}{|\lambda_{(m-1)_0}|}\left(\frac{dz_{m-1}}{d\tau} + \widetilde{\mathbf{v}}_{m-1} \sum_{j=1}^{n} \frac{d\mathbf{v}_j}{d\tau} z_j\right) &= -\widetilde{\lambda}_{(m-1)} z_{m-1} + \frac{1}{|\lambda_{(m-1)_0}|}(\widetilde{\mathbf{v}}_{m-1} \mathbf{g}), \\
\frac{dz_m}{d\tau} + \widetilde{\mathbf{v}}_m \sum_{j=1}^{n} \frac{d\mathbf{v}_j}{d\tau} z_j &= -\widetilde{\lambda}_{(m)} z_m + \frac{1}{|\lambda_{(m)_0}|}(\widetilde{\mathbf{v}}_m \mathbf{g}), \qquad (2.20) \\
\varepsilon\left(\frac{dz_{m+1}}{d\tau} + \widetilde{\mathbf{v}}_{m+1} \sum_{j=1}^{n} \frac{d\mathbf{v}_j}{d\tau} z_j\right) &= -\widetilde{\lambda}_{(m+1)} z_{m+1} + \frac{1}{|\lambda_{(m+1)_0}|}(\widetilde{\mathbf{v}}_{m+1} \mathbf{g}), \\
\varepsilon\left(\frac{dz_{m+2}}{d\tau} + \widetilde{\mathbf{v}}_{m+2} \sum_{j=1}^{n} \frac{d\mathbf{v}_j}{d\tau} z_j\right) &= \frac{|\lambda_{(m+2)_0}|}{|\lambda_{(m+1)_0}|}\Big(- \widetilde{\lambda}_{(m+2)} z_{m+2} + \\
&\quad \frac{1}{|\lambda_{(m+2)_0}|}(\widetilde{\mathbf{v}}_{m+1} \mathbf{g})\Big), \\
&\vdots \\
\varepsilon\left(\frac{dz_n}{d\tau} + \widetilde{\mathbf{v}}_n \sum_{j=1}^{n} \frac{d\mathbf{v}_j}{d\tau} z_j\right) &= \frac{|\lambda_{(n)_0}|}{|\lambda_{(m+1)_0}|}\Big(- \widetilde{\lambda}_{(n)} z_n + \frac{1}{|\lambda_{(n)_0}|}(\widetilde{\mathbf{v}}_n \mathbf{g})\Big),
\end{aligned}$$

Once again, the system (2.20) constitutes a singular perturbation problem, with ε as a small parameter. It should be noted that it is the ratio $\varepsilon = |\lambda_{(m)_0}|/|\lambda_{(m+1)_0}| \ll 1$ that represents the small parameter, while $|\lambda_{(m)_0}|$ and $|\lambda_{(m+1)_0}|$ may be of any order. Now, taking the limit $\varepsilon \to 0$, $\tau \gtrsim 1$, one can write:

$$\begin{aligned}
\frac{|\lambda_{(m)_0}|}{|\lambda_{(1)_0}|}\left(\frac{dz_1}{d\tau} + \widetilde{\mathbf{v}}_1 \sum_{j=1}^{n} \frac{d\mathbf{v}_j}{d\tau} z_j\right) &= -\widetilde{\lambda}_{(1)} z_1 + \frac{1}{|\lambda_{(1)_0}|}(\widetilde{\mathbf{v}}_1 \mathbf{g}), \\
&\vdots \\
\frac{|\lambda_{(m)_0}|}{|\lambda_{(m-1)_0}|}\left(\frac{dz_{m-1}}{d\tau} + \widetilde{\mathbf{v}}_{m-1} \sum_{j=1}^{n} \frac{d\mathbf{v}_j}{d\tau} z_j\right) &= -\widetilde{\lambda}_{(m-1)} z_{m-1} + \frac{1}{|\lambda_{(m-1)_0}|}(\widetilde{\mathbf{v}}_{m-1} \mathbf{g}), \\
\frac{dz_m}{d\tau} + \widetilde{\mathbf{v}}_m \sum_{j=1}^{n} \frac{d\mathbf{v}_j}{d\tau} z_j &= -\widetilde{\lambda}_{(m)} z_m + \frac{1}{|\lambda_{(m)_0}|}(\widetilde{\mathbf{v}}_m \mathbf{g}), \qquad (2.21) \\
0 &= -\widetilde{\lambda}_{(m+1)} z_{m+1} + \frac{1}{|\lambda_{(m+1)_0}|}(\widetilde{\mathbf{v}}_{m+1} \mathbf{g}),
\end{aligned}$$

$$
\begin{aligned}
0 &= \frac{|\lambda_{(m+2)_0}|}{|\lambda_{(m+1)_0}|}\Big(-\widetilde{\lambda}_{(m+2)} z_{m+2} + \\
&\quad \frac{1}{|\lambda_{(m+2)_0}|}(\widetilde{\mathbf{v}}_{m+1}\mathbf{g})\Big), \\
&\vdots \\
0 &= \frac{|\lambda_{(n)_0}|}{|\lambda_{(m+1)_0}|}\Big(-\widetilde{\lambda}_{(n)} z_n + \frac{1}{|\lambda_{(n)_0}|}(\widetilde{\mathbf{v}}_n\mathbf{g})\Big),
\end{aligned}
$$

or in terms of the original variables one can rewrite (2.21) as:

$$
\begin{aligned}
\widetilde{\mathbf{v}}_s \frac{d\mathbf{y}}{dt} &= \widetilde{\mathbf{v}}_s\mathbf{f}, \\
\mathbf{0} &= \widetilde{\mathbf{v}}_f\mathbf{f},
\end{aligned}
\tag{2.22}
$$

which coincides with the result obtained by Maas and Pope [15]. Therefore, it is proved that there exists a neighborhood of the equilibrium point where the system (2.1) can be replaced with the reduced system (2.22) for $t \gtrsim 1/|\lambda_{m_0}|$ if $\varepsilon = |\lambda_{(m)_0}|/|\lambda_{(m+1)_0}| \ll 1$. Moreover, since the the solution of the second equation of the system (2.22) does not depend on the initial conditions, it represents an attracting manifold. It should be noted that the requirement of the small neighborhood of the equilibrium point is due to restriction on $\widetilde{\lambda}_{(i)}$ to be of the order of 1, hence if $\widetilde{\lambda}_{(i)}$ are weak functions of $\mathbf{y}$, the requirement of a small neighborhood can be taken away, and so the reduced system (2.22) can be used far from the equilibrium point. As it was mentioned while considering the linear case, there are two errors associated with the technique: solution approximation error and error of approximation of the slow manifold by the ILDM. The important distinction with the linear case is that for general form of $\mathbf{f}$, the ILDM does not represent a solution of the original system and hence we have nonzero error of approximating the SM by the ILDM.

2.1.3 Nonlinear systems with k spectral gaps

Here, we generalize the results of the previous section to consider systems with an arbitrary number of gaps in the eigenvalue spectrum; that is, we suppose:

$$\begin{aligned} \varepsilon_{m_1} &= \frac{|\lambda^{(0)}_{(m_1)}|}{|\lambda^{(0)}_{(m_1+1)}|} \ll 1, \\ &\vdots \\ \varepsilon_{m_k} &= \frac{|\lambda^{(0)}_{(m_k)}|}{|\lambda^{(0)}_{(m_k+1)}|} \ll 1, \qquad k < n. \end{aligned} \tag{2.23}$$

Now, repeating the steps from the previous section we obtain:

$$\frac{1}{|\lambda^{(0)}_{(i)}|}\left(\frac{dz_i}{dt} + \widetilde{\mathbf{v}}_i \sum_{j=1}^{n} \frac{d\mathbf{v}_j}{dt} z_j\right) = -\widetilde{\lambda}_{(i)} z_1 + \frac{1}{|\lambda^{(0)}_{(i)}|}(\widetilde{\mathbf{v}}_i \mathbf{g}), \qquad i = 1, \ldots, n. \tag{2.24}$$

Further, following the development of the previous section, we consider the system above separately on the following time intervals:

$$\begin{aligned} \triangle_0 &= \left\{ t: \quad 0 \le t \lesssim \frac{1}{|\lambda^{(0)}_{(m_k)}|} \right\}, \\ \triangle_1 &= \left\{ t: \quad \frac{1}{|\lambda^{(0)}_{(m_k)}|} \lesssim t \lesssim \frac{1}{|\lambda^{(0)}_{(m_{k-1})}|} \right\}, \\ &\vdots \\ \triangle_{k-1} &= \left\{ t: \quad \frac{1}{|\lambda^{(0)}_{(m_2)}|} \lesssim t \lesssim \frac{1}{|\lambda^{(0)}_{(m_1)}|} \right\}, \\ \triangle_k &= \left\{ t: \quad t \gtrsim \frac{1}{|\lambda^{(0)}_{(m_1)}|} \right\}. \end{aligned} \tag{2.25}$$

On $\triangle_0$ we rescale time variable $\tau = t\lambda^{(0)}_{(m_k)}/\varepsilon_{(m_k)}$ to obtain:

$$\begin{aligned} \frac{|\lambda_{(m)_0}|}{|\lambda_{(1)_0}|}\left(\frac{dz_1}{d\tau} + \widetilde{\mathbf{v}}_1 \sum_{j=1}^{n} \frac{d\mathbf{v}_j}{d\tau} z_j\right) &= \varepsilon_{m_k}\left(-\widetilde{\lambda}_{(1)} z_1 + \frac{1}{|\lambda_{(1)_0}|}(\widetilde{\mathbf{v}}_1 \mathbf{g})\right), \\ &\vdots \\ \frac{|\lambda_{(m)_0}|}{|\lambda_{(m-1)_0}|}\left(\frac{dz_{m-1}}{d\tau} + \widetilde{\mathbf{v}}_{m-1} \sum_{j=1}^{n} \frac{d\mathbf{v}_j}{d\tau} z_j\right) &= \varepsilon_{m_k}\left(-\widetilde{\lambda}_{(m-1)} z_{m-1} + \frac{1}{|\lambda_{(m-1)_0}|}(\widetilde{\mathbf{v}}_{m-1} \mathbf{g})\right), \end{aligned}$$

$$
\begin{aligned}
\frac{dz_m}{d\tau} + \widetilde{\mathbf{v}}_m \sum_{j=1}^{n} \frac{d\mathbf{v}_j}{d\tau} z_j &= \varepsilon_{m_k} \Big(- \widetilde{\lambda}_{(m)} z_m + \frac{1}{|\lambda_{(m)_0}|} \Big) (\widetilde{\mathbf{v}}_m \mathbf{g}), \qquad (2.26) \\
\frac{dz_{m+1}}{d\tau} + \widetilde{\mathbf{v}}_{m+1} \sum_{j=1}^{n} \frac{d\mathbf{v}_j}{d\tau} z_j &= - \widetilde{\lambda}_{(m+1)} z_{m+1} + \frac{1}{|\lambda_{(m+1)_0}|} (\widetilde{\mathbf{v}}_{m+1} \mathbf{g}), \\
\frac{dz_{m+2}}{d\tau} + \widetilde{\mathbf{v}}_{m+2} \sum_{j=1}^{n} \frac{d\mathbf{v}_j}{d\tau} z_j &= \frac{|\lambda_{(m+2)_0}|}{|\lambda_{(m+1)_0}|} - \widetilde{\lambda}_{(m+2)} z_{m+2} + \\
& \qquad \frac{1}{|\lambda_{(m+2)_0}|} (\widetilde{\mathbf{v}}_{m+1} \mathbf{g}), \\
& \vdots \\
\frac{dz_n}{d\tau} + \widetilde{\mathbf{v}}_n \sum_{j=1}^{n} \frac{d\mathbf{v}_j}{d\tau} z_j \Big) &= \frac{|\lambda_{(n)_0}|}{|\lambda_{(m+1)_0}|} - \widetilde{\lambda}_{(n)} z_n + \frac{1}{|\lambda_{(n)_0}|} (\widetilde{\mathbf{v}}_n \mathbf{g}),
\end{aligned}
$$

or after neglecting the terms of the order of ε_{m_k} and returning to the original variables:

$$
\begin{aligned}
\widetilde{\mathbf{v}}_s^{(m_k)} \frac{d\mathbf{y}}{dt} &= \mathbf{0}, \qquad (2.27) \\
\widetilde{\mathbf{v}}_f^{(m_k)} \frac{d\mathbf{y}}{dt} &= \widetilde{\mathbf{v}}_f^{(m_k)} \mathbf{f}.
\end{aligned}
$$

On $\triangle_l, l = 1, \ldots, k$, we rescale time variable $\tau = t\lambda_{(m_k)^{(0)}}$ to obtain:

$$
\begin{aligned}
\frac{|\lambda_{(m)_0}|}{|\lambda_{(1)_0}|} \Big(\frac{dz_1}{d\tau} + \widetilde{\mathbf{v}}_1 \sum_{j=1}^{n} \frac{d\mathbf{v}_j}{d\tau} z_j \Big) &= - \widetilde{\lambda}_{(1)} z_1 + \frac{1}{|\lambda_{(1)_0}|} (\widetilde{\mathbf{v}}_1 \mathbf{g}), \\
& \vdots \\
\frac{|\lambda_{(m)_0}|}{|\lambda_{(m-1)_0}|} \Big(\frac{dz_{m-1}}{d\tau} + \widetilde{\mathbf{v}}_{m-1} \sum_{j=1}^{n} \frac{d\mathbf{v}_j}{d\tau} z_j \Big) &= - \widetilde{\lambda}_{(m-1)} z_{m-1} + \frac{1}{|\lambda_{(m-1)_0}|} (\widetilde{\mathbf{v}}_{m-1} \mathbf{g}), \\
\frac{dz_m}{d\tau} + \widetilde{\mathbf{v}}_m \sum_{j=1}^{n} \frac{d\mathbf{v}_j}{d\tau} z_j &= - \widetilde{\lambda}_{(m)} z_m + \frac{1}{|\lambda_{(m)_0}|} (\widetilde{\mathbf{v}}_m \mathbf{g}), \qquad (2.28) \\
\varepsilon_{m_k} \Big(\frac{dz_{m+1}}{d\tau} + \widetilde{\mathbf{v}}_{m+1} \sum_{j=1}^{n} \frac{d\mathbf{v}_j}{d\tau} z_j \Big) &= - \widetilde{\lambda}_{(m+1)} z_{m+1} + \frac{1}{|\lambda_{(m+1)_0}|} (\widetilde{\mathbf{v}}_{m+1} \mathbf{g}), \\
\varepsilon_{m_k} \Big(\frac{dz_{m+2}}{d\tau} + \widetilde{\mathbf{v}}_{m+2} \sum_{j=1}^{n} \frac{d\mathbf{v}_j}{d\tau} z_j \Big) &= \frac{|\lambda_{(m+2)_0}|}{|\lambda_{(m+1)_0}|} \Big(- \widetilde{\lambda}_{(m+2)} z_{m+2} + \\
& \qquad \frac{1}{|\lambda_{(m+2)_0}|} (\widetilde{\mathbf{v}}_{m+1} \mathbf{g}) \Big), \\
& \vdots
\end{aligned}
$$

$$\varepsilon_{m_k}\left(\frac{dz_n}{d\tau}+\widetilde{\mathbf{v}}_n\sum_{j=1}^{n}\frac{d\mathbf{v}_j}{d\tau}z_j\right) = \frac{|\lambda_{(n)_0}|}{|\lambda_{(m+1)_0}|}\left(-\widetilde{\lambda}_{(n)}z_n+\frac{1}{|\lambda_{(n)_0}|}(\widetilde{\mathbf{v}}_n\mathbf{g})\right),$$

and after neglecting the terms of the order of ε_{m_k}:

$$\begin{aligned}
\frac{|\lambda_{(m)_0}|}{|\lambda_{(1)_0}|}\left(\frac{dz_1}{d\tau}+\widetilde{\mathbf{v}}_1\sum_{j=1}^{n}\frac{d\mathbf{v}_j}{d\tau}z_j\right) &= -\widetilde{\lambda}_{(1)}z_1+\frac{1}{|\lambda_{(1)_0}|}(\widetilde{\mathbf{v}}_1\mathbf{g}),\\
&\vdots\\
\frac{|\lambda_{(m)_0}|}{|\lambda_{(m-1)_0}|}\left(\frac{dz_{m-1}}{d\tau}+\widetilde{\mathbf{v}}_{m-1}\sum_{j=1}^{n}\frac{d\mathbf{v}_j}{d\tau}z_j\right) &= -\widetilde{\lambda}_{(m-1)}z_{m-1}+\frac{1}{|\lambda_{(m-1)_0}|}(\widetilde{\mathbf{v}}_{m-1}\mathbf{g}),\\
\frac{dz_m}{d\tau}+\widetilde{\mathbf{v}}_m\sum_{j=1}^{n}\frac{d\mathbf{v}_j}{d\tau}z_j &= -\widetilde{\lambda}_{(m)}z_m+\frac{1}{|\lambda_{(m)_0}|}(\widetilde{\mathbf{v}}_m\mathbf{g}), \qquad (2.29)\\
0 &= -\widetilde{\lambda}_{(m+1)}z_{m+1}+\frac{1}{|\lambda_{(m+1)_0}|}(\widetilde{\mathbf{v}}_{m+1}\mathbf{g}),\\
0 &= \frac{|\lambda_{(m+2)_0}|}{|\lambda_{(m+1)_0}|}\left(-\widetilde{\lambda}_{(m+2)}z_{m+2}+\right.\\
&\quad \left.\frac{1}{|\lambda_{(m+2)_0}|}(\widetilde{\mathbf{v}}_{m+1}\mathbf{g})\right),\\
&\vdots\\
0 &= \frac{|\lambda_{(n)_0}|}{|\lambda_{(m+1)_0}|}\left(-\widetilde{\lambda}_{(n)}z_n+\frac{1}{|\lambda_{(n)_0}|}(\widetilde{\mathbf{v}}_n\mathbf{g})\right),
\end{aligned}$$

or in terms of the original variables one can rewrite (2.21) as:

$$\begin{aligned}
\widetilde{\mathbf{v}}_s^{(m_k)}\frac{d\mathbf{y}}{dt} &= \widetilde{\mathbf{v}}_s^{(m_k)}\mathbf{f} \qquad (2.30)\\
0 &= \widetilde{\mathbf{v}}_f^{(m_k)}\mathbf{f},
\end{aligned}$$

Therefore, on each time interval $\triangle_l, l = 1,\ldots,k$, a system can be approximated by the ILDMs of the orders of $k,\ldots,k-(l-1)$; that is, it consequently goes through ILDMs of progressively lower dimension. Obviously, this hierarchy can be incomplete in a sense that the solution can be approximated by the ILDMs of orders of i_1 and i_2, while cannot be approximated by the ILDM of the order of i, where $i_1 < i < i_2$. Presence of a spectral gap for some i provides a sufficient condition for the approximation by the ILDM of the order of i to be possible.

Now, let us consider two ILDMs of different dimensions:

$$\widetilde{\mathbf{v}}_f^{(m_1)}\mathbf{f} = \mathbf{0}, \tag{2.31}$$

$$\widetilde{\mathbf{v}}_f^{(m_2)}\mathbf{f} = \mathbf{0}, \tag{2.32}$$

where $m_2 > m_1$. The system (2.31) coincides with the system (2.32), but has $(m_2 - m_1)$ additional equations. Therefore, any solution of the system (2.31) represents a solution of the system (2.32) as well. Geometrically, it means that each ILDM contains all the ILDMs of lower dimensions.

2.1.4 Notions on the error for the nonlinear systems

In the nonlinear case it seems impossible to derive a general formula giving the error of the approximation of the original system (2.1) with an arbitrary source function $\mathbf{f}(\mathbf{y})$ by the reduced system (2.22). Indeed, some features can be seen on the following example, introduced by Davis and Skodje [7]:

$$\frac{dx}{dt} = -x, \tag{2.33}$$

$$\frac{dy}{dt} = -\gamma y + \frac{(\gamma-1)x + \gamma x^2}{(1+x)^2}, \tag{2.34}$$

where $\gamma > 1$. The system (2.33) has a stable source type equilibrium point at the origin. The exact solution is given by:

$$x(t) = x_0 e^{-t}, \tag{2.35}$$

$$y(t) = \left(y_0 - \frac{x_0}{1+x_0}\right)e^{-\gamma t} + \frac{x_0 e^{-t}}{1+x_0 e^{-t}}, \tag{2.36}$$

where x_0 and y_0 are the initial conditions. In the phase plane this is:

$$y(x) = \left(y_0 - \frac{x_0}{1+x_0}\right)\left(\frac{x}{x_0}\right)^{\gamma} + \frac{x}{1+x}. \tag{2.37}$$

A solution of the system (2.33) starts from (x_0, y_0) and moves toward the equilibrium point first approaching the slow manifold:

$$y_{sm} = \frac{x}{1+x}. \tag{2.38}$$

To find the ILDM approximation, we first find the Jacobian matrix:

$$\mathbf{J} = \begin{pmatrix} -1 & 0 \\ \frac{\gamma-1+(\gamma+1)x}{(1+x)^3} & -\gamma \end{pmatrix}. \tag{2.39}$$

The Jordan decomposition of (2.39) is given by:

$$\mathbf{V}\mathbf{\Lambda}\widetilde{\mathbf{V}} = \begin{pmatrix} 1 & 0 \\ \frac{\gamma-1+(\gamma+1)y_1}{(\gamma-1)(1+y_1)^3} & 1 \end{pmatrix} \begin{pmatrix} -1 & 0 \\ 0 & -\gamma \end{pmatrix} \begin{pmatrix} 1 & 0 \\ -\frac{\gamma-1+(\gamma+1)y_1}{(\gamma-1)(1+y_1)^3} & 1 \end{pmatrix}. \tag{2.40}$$

The ILDM approximation here is obtained from equation (2.22) by setting to 0 the dot product of the inverse eigenvector corresponding to the most negative eigenvalue and the vector representing the right hand side of the system (2.33). Here, it can be written in a closed form:

$$y_{ildm}(x) = \frac{x}{1+x} + \frac{2x^2}{\gamma(\gamma-1)(1+x^2)}. \tag{2.41}$$

The error of the approximation of the slow manifold by the ILDM is given by:

$$E_{sm} = |y_{sm} - y_{ildm}| = \frac{2x^2}{\gamma(\gamma-1)(1+x^2)}. \tag{2.42}$$

The ILDM method neglects terms $o(\gamma^0)$, and in this example the error is $O(1/\gamma^2)$. According to the theory developed in the previous sections, the ILDM (2.41) can be used to approximate the solution of the original system (2.33) for $t \gtrsim 1$, in which case we have:

$$\tilde{x} = x_0 e^{-t}, \tag{2.43}$$

$$\tilde{y} = \frac{x_0 e^{-t}}{1 + x_0 e^{-t}} + \frac{2x_0^2 e^{-2t}}{\gamma(\gamma-1)(1+x_0 e^{-t})^3}. \tag{2.44}$$

Here the ILDM method approximation does not depend on the initial condition for y, the result which could be expected from the form of the exact solution (2.35). The solution for x coincides with the exact solution, which is, of course, the consequence

of the first equation being decoupled and is not true in general. The error of the approximation of y is given by:

$$\begin{aligned} E_y &= |y - \tilde{y}| \\ &= \left| \left(y_0 - \frac{x_0}{1+x_0} \right) e^{-\gamma t} - \frac{2x_0^2 e^{-2t}}{\gamma(\gamma-1)(1+x_0 e^{-t})^3} \right| \\ &\leq \left| y_0 - \frac{x_0}{1+x_0} \right| e^{-\gamma} + \frac{2x_0^2 e^{-2}}{\gamma(\gamma-1)}. \end{aligned} \tag{2.45}$$

The first term in the (2.45) accounts for the error of approximation of the exact solution by the slow manifold, and goes to 0 exponentially as the stiffness increases. The second term accounts for the error of the approximation of the slow manifold by the ILDM and goes to 0 as $1/\gamma^2$. Therefore, in this example the biggest error comes from the approximation of the slow manifold by the ILDM. We expect this situation to be true in general, and hence the total error of the method can be significantly decreased by improving the approximation of the slow manifold. One can use the ILDM as an initial guess in the iteration kind of methods like those developed by Roussel and Fraser [20]. The idea of using the ILDM as an intial guess was originally offered by Davis and Skodje [7].

2.1.5 Using the Schur decomposition instead of the Jordan decomposition

In their original paper Maas and Pope [15] offered to use the Schur decomposition instead of the Jordan decomposition to avoid numerical difficulties, which may arise due to poor conditioning. The Schur formulation has the advantage of orthogonality of the basis vectors. In this section we will prove the equivalence of both formulations.

The Schur decomposition is expressed by the following formula:

$$\mathbf{J} = \mathbf{Q}\mathbf{T}\mathbf{Q}^T, \tag{2.46}$$

where

$$\mathbf{Q} = \left(\begin{array}{ccc|ccc} | & & | & | & & | \\ \mathbf{q}_1 & \cdots & \mathbf{q}_m & \mathbf{q}_{m+1} & \cdots & \mathbf{q}_n \\ | & & | & | & & | \end{array} \right) = \left(\begin{array}{c|c} \mathbf{Q}_s & \mathbf{Q}_f \end{array} \right) \tag{2.47}$$

$$\mathbf{T} = \begin{pmatrix} \lambda_{(1)} & t_{12} & \dots & t_{1n} \\ 0 & \lambda_{(1)} & \dots & t_{2n} \\ 0 & \dots & \ddots & \vdots \\ 0 & \dots & 0 & \lambda_{(n)} \end{pmatrix} \tag{2.48}$$

$$\mathbf{Q}^T = \left(\begin{array}{ccc} - & \mathbf{q}_1^T & - \\ & \vdots & \\ - & \mathbf{q}_m^T & - \\ \hline - & \mathbf{q}_{m+1}^T & - \\ & \vdots & \\ - & \mathbf{q}_n^T & - \end{array} \right) = \left(\begin{array}{c} \mathbf{Q}_s^T \\ \hline \mathbf{Q}_f^T \end{array} \right) \tag{2.49}$$

Here, $\mathbf{Q}$ is an orthogonal matrix with Schur vectors in its columns, $\mathbf{T}$ is an upper triangular matrix with the eigenvalues of $\mathbf{J}$ along its main diagonal. Again it is important that the eigenvalues are ordered from the least negative to the most negative, and $\mathbf{Q}^T$ is a transposed Schur vector matrix with Schur vectors in its rows.

Here, we prove that the reduced system (2.22) expressed in terms of eigenvectors is equivalent to the following system expressed in terms of Schur vectors:

$$\mathbf{Q}_s^T \frac{d\mathbf{y}}{dt} = \mathbf{Q}_s^T \mathbf{f} \tag{2.50}$$

$$0 = \mathbf{Q}_f^T \mathbf{f}. \tag{2.51}$$

Proof:

$$\mathbf{JQ} = \mathbf{QT} \quad \Leftrightarrow \quad \mathbf{Jq}_i = \mathbf{Qt}_i = \mathbf{q}_i \lambda_i + \sum_{k=1}^{i-1} \mathbf{q}_k t_{ki} \quad \Rightarrow$$

$$
\begin{aligned}
i = 1: \qquad & \mathbf{J}\mathbf{q}_1 = \mathbf{q_1}\lambda_1 \quad \Rightarrow \quad \mathbf{q}_1 = C_1\mathbf{v}_1 \\
i = 2: \qquad & \mathbf{J}\mathbf{q}_2 = \mathbf{q}_2\lambda_2 + \mathbf{q}_1 t_{12} \quad \Rightarrow \quad \mathbf{q}_2 = C_2\mathbf{v}_2 + \frac{t_{12}}{(\lambda_1 - \lambda_2)}\mathbf{q}_1 \\
i = 3: \qquad & \mathbf{J}\mathbf{q}_3 = \mathbf{q}_3\lambda_3 + \mathbf{q}_1 t_{13} + \mathbf{q}_2 t_{23} \quad \Rightarrow \\
& \mathbf{q}_3 = C_3\mathbf{v}_2 + \frac{t_{13}}{(\lambda_1 - \lambda_3)}\mathbf{q}_1 + \frac{t_{23}}{(\lambda_2 - \lambda_3)}\mathbf{q}_2, \quad etc.
\end{aligned}
$$

Here C_i are constants, $\mathbf{t}_i$ are the columns of $\mathbf{T}$. Continuing this process till $i = m$ one can see that $\mathbf{q}_i$, $i = 1, \ldots, m$, are the linear combinations of $\mathbf{v}_i$, $i = 1, \ldots, m$, and hence they span the same m-dimensional subspace. Further, since

$$\widetilde{\mathbf{v}}_i \cdot \mathbf{v}_j = \delta_{ij},$$

then $\widetilde{\mathbf{v}}_i$, $i = 1, \ldots, m$, belongs to the same subspace. The same is true for $\mathbf{q}_i^T$, $i = 1, \ldots, m$, which follows from the definition of the orthogonal matrix. Therefore, $\widetilde{\mathbf{V}}_s$ and $\mathbf{Q}_s^T$ consist of the vectors, which span the same m-dimensional subspace, and hence there exists a nontrivial $m \times n$ matrix $\mathbf{L}$ such that:

$$\mathbf{L}\widetilde{\mathbf{V}}_s = \mathbf{Q}_s^T, \tag{2.52}$$

which proves the proposition.

2.2 Numerical solution

The second of the Maas-Pope equations (2.22)

$$\widetilde{\mathbf{V}}_f \mathbf{f} = \mathbf{0} \tag{2.53}$$

represents an algebraic system of $(n - m)$ equations with n unknowns and defines an m-dimensional surface in the n-dimensional phase space. The surface defined by that equation is referred to by Maas and Pope [15] as the ILDM. Equation (2.53) is solved in some predetermined domain of the n- dimensional phase space. The solution is stored in a table parameterized by m chosen variables, and is used to integrate the system (2.22). This section concerns a numerical procedure that can be used to solve the equation (2.53).

2.2.1 One-dimensional ILDM

In the case of a one-dimensional ILDM we have $m = 1$. That physically means that the equilibrium point of the original system (2.1) has one distinctive slow time scale. Equation (2.53) becomes an algebraic system of $n - 1$ equations with n unknowns and hence defines a curve in the n- dimensional phase space.

To compute the curve, one can chose one of the state variables y_i as a parameter, which makes the system closed, and solve the equation (2.53) for some range of the chosen parameter. This choice is somewhat arbitrary; however, given an improper choice of the parameter, numerical difficulties due to the shape of the curve may arise. We will discuss those difficulties later, and for now suppose that we have made a proper choice of the parameter and closed the system (2.53). Now, one can start from a known point on the ILDM, give an increment to the parameter and compute next point using the values of the other state variables at the known point as an initial guess for Newton's method. The only point on the ILDM which is known *a priori* is the equilibrium point, and so for the first computed point we have the

following:

$$\begin{aligned} \mathbf{0} &= \widetilde{\mathbf{V}}_f(\mathbf{y})\mathbf{f}(\mathbf{y}), \\ y_p &= y_{p_{eq}} + \triangle y_p = \text{fixed}, \\ y_{i_{in}} &= y_{i_{eq}}, \quad i \neq p. \end{aligned} \tag{2.54}$$

Here, y_p is a variable chosen as the parameter, $y_{p_{eq}}$ is the value of the parameter at the equilibrium point, $\triangle y_p$ is the parameter change, $y_{i_{in}}$, $i = 1, \cdots, n, i \neq p$ are initial guesses for the variables other than the parameter, and $y_{i_{eq}}$ are the values of those variables at the equilibrium point. Use of an adjacent point as an initial guess virtually guarantees quick convergence; however, direct application of Newton's method requires recomputing of the $\widetilde{\mathbf{V}}_f(\mathbf{y})$ at each iteration and makes solution computationally expensive. To avoid recomputation of the $\widetilde{\mathbf{V}}_f(\mathbf{y})$ and hence to reduce computational time, the system (2.54) is often replaced with the following one:

$$\begin{aligned} \mathbf{0} &= \widetilde{\mathbf{V}}_f(\mathbf{y}_{in})\mathbf{f}(\mathbf{y}) \\ y_p &= y_{p_{eq}} + \triangle y_p = \text{fixed} \\ y_{i_{in}} &= y_{i_{eq}}, \quad i \neq p. \end{aligned} \tag{2.55}$$

This system is solved using a standard Newton's method, and the solution is used as an initial guess to compute next point on the ILDM. Replacement of the system (2.54) with the system (2.55) gives rise to the error of approximation of the ILDM by simplified system (2.55). This error of such approximation can be estimated by the following formula:

$$E_{ILDM} = \max_i |\widetilde{V}_{f_{i,j}} f_j|. \tag{2.56}$$

In their original paper, Maas and Pope [15] demonstrated the importance of proper parametrization on a simple example shown on the Fig. 2.1. It shows an

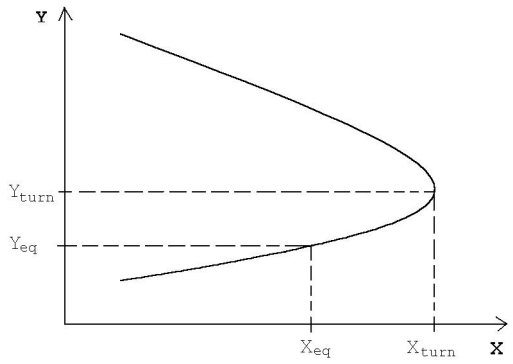

Figure 2.1. Parameterization failure example

arbitrary example of a one-dimensional manifold in the two-dimensional space. Here, if x is chosen as a parameter, the method fails near the turning point; however, if y is chosen as a parameter, the problem can be easily solved. Generally, the problem arises not only near turning points, but every time when the derivatives with respect to chosen parameter are high. Maas and Pope offered to use arc length continuation method to avoid this problem. Here, we consider a different technique, which uses optimal choice of a parameter at each point. First, we rewrite the first equation of the system (2.55) as follows:

$$\widetilde{\mathbf{V}}_f(\mathbf{y}_{in})\mathbf{f}(\mathbf{y}) = \mathbf{G}(\mathbf{y}) = 0 \quad \Leftrightarrow \quad \begin{cases} g_1(y_1, \ldots, y_n) &= 0 \\ &\vdots \\ g_{n-1}(y_1, \ldots, y_n) &= 0 \end{cases} \tag{2.57}$$

Further, we note that each of the equations of the system (2.57) represents a surface in the n-dimensional space, and the one-dimensional ILDM can be locally obtained as the crossing of those surfaces. It immediately follows that the local tangent to the ILDM is locally given as the crossing of the tangent planes to the surfaces defined by the system (2.57). Further, we linearize (2.57) to obtain:

$$A_{11}y_1 + \ldots + A_{1n}y_n + A_{10} = 0$$

$$\vdots \qquad (2.58)$$

$$A_{(n-1)1}y_1 + \ldots + A_{(n-1)n}y_n + A_{(n-1)0} = 0$$

Equations (2.58) give tangent planes to the surfaces defined by the system (2.57). $(A_{i1}, \ldots, A_{in})$ are known from linear algebra to give the normal vectors to the i-th plane defined by (2.58). Since a local tangent to the ILDM is a line which belongs to all those planes, it is orthogonal to all the vectors $(A_{i1}, \ldots, A_{in}), \quad i = 1, \ldots, n-1$. This result can be expressed as follows:

$$\begin{pmatrix} A_{11} & \ldots & A_{1n} \\ \ldots & \ldots & \ldots \\ A_{(n-1)1} & \ldots & A_{(n-1)n} \end{pmatrix} \begin{pmatrix} T_1 \\ \ldots \\ T_n \end{pmatrix} = \mathbf{0}, \qquad (2.59)$$

where T_i are the components of the tangent vector. The solution of the system (2.59) is given by the following determinant:

$$\mathbf{T} = \begin{vmatrix} \mathbf{e}_1 & \ldots & \mathbf{e}_n \\ A_{11} & \ldots & A_{1n} \\ \ldots & \ldots & \ldots \\ A_{(n-1)1} & \ldots & A_{(n-1)n} \end{vmatrix}, \qquad (2.60)$$

where $\mathbf{e}_1, \ldots, \mathbf{e}_n$ are orthogonal unit vectors associated with coordinate axes. The last result is a simple generalization of that in the three-dimensional space and is easily proven by direct substitution. One can compute the components of the vector tangent to the ILDM from the formula (2.60) and use the state variable y_p that corresponds to the component of tangent vector having maximum absolute value. This choice of the parameter automatically solves the problem with the turning points and moreover gives smaller error of approximation of the ILDM by (2.55) in comparison with the other choices of the parameter, because a computed point is located as close to the starting point as it allowed by the choice of the increment $\triangle y_p$.

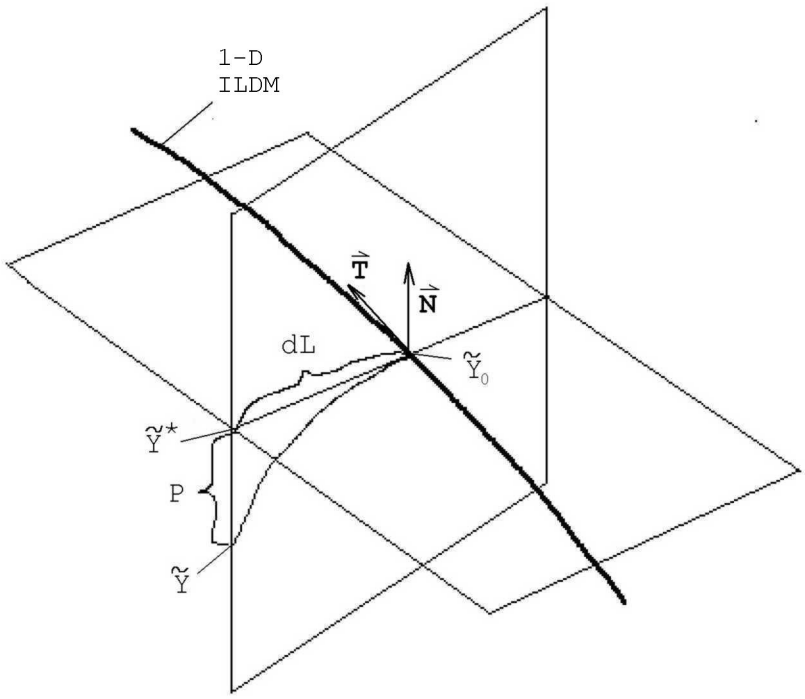

Figure 2.2. Parameterization of a two-dimensional ILDM

2.2.2 Two-dimensional ILDM

In section 2.1.3 it was shown that there exists a hierarchy of ILDMs of different orders; that is, one-dimensional ILDMs belong to two-dimensional ILDMs and so on. This fact can be used to compute the ILDM of the second order. To do so, one can subdivide the one-dimensional ILDM into small intervals and at each point of that subdivision advance in both directions following the procedure outlined in Fig. 2.2. Here, $\widetilde{\mathbf{Y}}_0$ is a point of subdivision of the three-dimensional projection of one-dimensional ILDM, $\mathbf{T}$ represents a unit vector tangent to the one-dimensional ILDM, $\mathbf{N}$ gives a unit vector normal to the two-dimensional ILDM, dL is a distance of advancement from the starting point and is directed along the line of intersection of the planes normal to one-dimensional and two-dimensional ILDMs, $\widetilde{\mathbf{Y}}^*$ is given

by the following formula:

$$\widetilde{\mathbf{Y}}^* = \widetilde{\mathbf{Y}}_0 + dL[\mathbf{N} \times \mathbf{T}], \tag{2.61}$$

and $\widetilde{\mathbf{Y}}$ is a point on the three dimensional projection of the two-dimensional ILDM to be computed. $\widetilde{\mathbf{Y}}$ is linked to $\widetilde{\mathbf{Y}}^*$ through the unknown parameter p by the formula:

$$\widetilde{\mathbf{Y}} = \widetilde{\mathbf{Y}}^* + \mathbf{N}p \tag{2.62}$$

Further, one can substitute (2.62) into the Maas-Pope formula to obtain a closed system. We use $p = 0$ as an initial guess for the variables constituting $\widetilde{\mathbf{Y}}$, while the values at the starting point are used as initial guesses for the other state variables. The most tricky part of this technique is computing of the normal vector to the two-dimensional ILDM. In the case of just three equations, the procedure is trivial and obtained by linearization of the only equation for two-dimensional ILDM. In the case of more than three dimensions, one needs to solve the linearized system to obtain the normal vector.

CHAPTER 3

GLUCOSE REGULATORY SYSTEM

In this chapter we apply the ILDM method to a model of the glucose regulatory system. The model introduced by Topp, *et al.* [24] incorporates β-cell mass, insulin and glucose dynamics, and gives rises to a stiff system of ODEs. The resulting system has two stable sink type equilibrium points and a saddle point. Both stable equilibria have two spectral gaps, and hence according to the theoretical results of the previous chapter, there exist both one- and two-dimensional slow manifolds. These manifolds are computed using numerical techniques developed above. In this chapter, we first describe the model, further present numerical results and finally give a stability analysis and consider defects in the regulatory system that give rise to diabetes.

3.1 Model

The description of the model presented in this section follows the original paper of Topp and co-workers [24].

3.1.1 Glucose dynamics

Glucose is released into the blood by the liver and kidneys, removed from the interstitial fluid by all the cells of the body, and distributed into many physiological compartments (e.g. arterial blood, venous blood, interstitial fluid). Experimental studies showed [1], [3] that despite such a complex distribution, slow glucose dynam-

ics (on a time scale of hours and larger) can be modeled using a one-compartment approximation. If one is concerned with the evolution of fasting blood glucose levels over a time scale of days to years, than glucose dynamics can be modeled by a single-compartment mass balance equation:

$$\frac{dG}{dt} = \text{Production} - \text{Uptake}, \tag{3.1}$$

where G is the concentration of glucose in the blood (measured in $\text{mg}\,\text{dl}^{-1}$), t is the time (measured in days), and Production and Uptake are the corresponding rates normalized by the volume of glucose distribution.

The rates of glucose production and uptake depend on blood glucose and insulin levels. These relationships were found experimentally [2] and can be written in the following form:

$$\text{Production} = P_0 - (E_{G0P} + S_{IP}I)G, \tag{3.2}$$

$$\text{Uptake} = U_0 + (E_{G0U} + S_{IU}I)G. \tag{3.3}$$

Here, P_0 and U_0 are the rates of glucose production and uptake at zero glucose, $E_{G0P} + S_{IP}I$ and $E_{G0U} + S_{IU}I$ are linear functions of insulin level and referred to as the glucose effectiveness parameters, E_{G0P} and E_{G0U} are glucose effectiveness at zero insulin, S_{IP} and S_{IU} are insulin sensitivity for production and uptake respectively, and I represents blood insulin concentration (measured in $\mu\text{U}\,\text{ml}^{-1}$)[1].

Using equations (3.2) and (3.3), one can rewrite (3.1) as follows:

$$\frac{dG}{dt} = R_0 - (E_{G0} + S_I I)G, \tag{3.4}$$

where $R_0 = P_0 - U_0$ is the net rate of production at zero glucose, $E_{G0} = E_{G0P} + E_{G0U}$ is the total glucose effectiveness at zero insulin, and $S_I = S_{IP} + S_{IU}$ is the total insulin sensitivity.

[1]Insulin is measured in units (U) (24 U=1 mg of pure insulin)

3.1.2 Insulin dynamics

Insulin is secreted by pancreatic β cells, cleared by the liver, kidneys, and insulin receptors, and distributed into several compartments (e.g. portal vein, peripheral blood, and interstitial fluid). Again, if one is concerned with the long-time evolution of fasting insulin levels in peripheral blood, then insulin dynamics is slow and can be approximated by a single-compartment equation:

$$\frac{dI}{dt} = \text{Secretion} - \text{Clearance}. \tag{3.5}$$

Here, Secretion and Clearance are rates normalized by insulin's volume of distribution ($\mu\text{U}\,\text{ml}^{-1}\,\text{d}^{-1}$).

The rate of insulin clearance is assumed to be proportional to blood insulin levels, that is:

$$\text{Clearance} = kI, \tag{3.6}$$

where k is a clearance constant which represents the combined insulin uptake at the liver, kidneys, and insulin receptors. This formula is exact when the system is near steady state; however, several studies showed that it also can be used to model more complex and relatively fast insulin dynamics (see for example [5]).

Experimantal [16] and analytical [6] studies showed that the net insulin secretion rate can be modeled as a sigmoidal function of glucose level, that is:

$$\text{Secretion} = \frac{\beta\sigma G^2}{\alpha + G^2}, \tag{3.7}$$

where β is the mass of pancreatic β cells (measured in mg). All β cells are assumed to secrete insulin at the same maximal rate σ (measured in ($\mu\text{U}\,\text{ml}^{-1}\,\text{d}^{-1}$), and $G^2/(\alpha+G^2)$ is a Hill function with coefficient 2 that describes a sigmoid ranging from 0 to 1 which reaches half its maximum at $G = \alpha^{1/2}$. Substituting equations (3.6) and (3.7) into equation (3.5), one obtains the equation governing insulin kinetics:

$$\frac{dI}{dt} = \frac{\beta\sigma G^2}{\alpha + G^2} - kI \tag{3.8}$$

3.1.3 β-cell mass dynamics

Despite a complex distribution of pancreatic β cells throughout the pancreas, β-cell mass dynamics can be approximated with a single- compartment model:

$$\frac{d\beta}{dt} = \text{Formation} - \text{Loss}, \tag{3.9}$$

where Formation and Loss represent the rates at which β-cell mass is added to or removed from the population, respectively.

New β cells can be formed by the replication of existing β cells, neogenesis (replication and differentiation) from stem cells, and transdifferentiation of other cells. In this model neogenesis and transdifferentiation are neglected, and hence Formation is assumed to be equal to Replication. This assumption is supported by several studies (see for example [11]), which indicate that neogenesis and transdifferentiation make a negligible contribution to β-cells mass dynamics except some special cases (such as a response to extreme physiological or chemically induced trauma).

Experimental studies show that the percentage of β cells undergoing replication varies as a nonlinear function of glucose level in the medium (see for example [13]). Replication rates for β cells increase with increasing glucose levels; however, at extreme hyperglycemia, β cell replication may be reduced. In the current model this behavior is modeled with a second-degree polynomial:

$$\text{Replication} = (r_{1r}G - r_{2r}G^2)\beta, \tag{3.10}$$

where r_{1r} (measured in $\text{mg}^{-1}\,\text{dl}\,\text{d}^{-1}$) and r_{2r} (measured in $\text{mg}^{-2}\,\text{dl}^2\,\text{d}^{-1}$)) are rate constants.

Cells can be lost from the β-cell mass by apostosis (regulated cell death), necrosis (unregulated cell death), or possibly transdifferentiation into othe types of endocrine cells. In the current model the rate of transdifferentiation is assumed to be negligible. Experimental studies show that death varies nonlinearly with glucose level (see for

example [9]. Increasing the glucose level reduces the rate of β-cell death, however starting from some value the rate either increases or remains unchanged. In the current model this behavior is modeled with a second-degree polynomial:

$$\text{Death} = (d_0 - r_{1a}G + r_{2a}G^2)\beta, \tag{3.11}$$

where d_0 is the death rate at zero glucose and r_{1a} (measured in $\text{mg}^{-1}\,\text{dl}\,\text{d}^{-1}$) and r_{2a} (measured in $\text{mg}^{-2}\,\text{dl}^2\,\text{d}^{-1}$) are constants. Substituting equations (3.10) and (3.11) into (3.9), one obtains the equation for β-cell mass dynamics:

$$\frac{d\beta}{dt} = (-d_0 + r_1 G - r_2 G^2)\beta, \tag{3.12}$$

where $r_1 = r_{1r} + r_{1a}$ and $r_2 = r_{2r} + r_{2a}$ are constants.

3.1.4 The system

Together, Equations (3.12), (3.8) and (3.4) constitute the glucose regulation model:

$$\begin{aligned} \frac{dG}{dt} &= R_0 - (E_{G0} + S_I I)G \\ \frac{dI}{dt} &= \frac{\beta\sigma G^2}{\alpha + G^2} - kI \\ \frac{d\beta}{dt} &= (-d_0 + r_1 G - r_2 G^2)\beta \end{aligned} \tag{3.13}$$

Values of the parameters corresponding to the normal human physiological state are presented in the table 3.1 [24]. For normal physiological values of the parameters the system (3.13) has three fixed points: ($G = 100\,\text{mg}\,\text{dl}^{-1}$, $I = 10\,\mu\text{U}\,\text{ml}^{-1}$, $\beta = 300\,\text{mg}$); ($G = 250\,\text{mg}\,\text{dl}^{-1}$, $I = 2.8\,\mu\text{U}\,\text{ml}^{-1}$, $\beta = 37\,\text{mg}$) and ($G = 600\,\text{mg}\,\text{dl}^{-1}$, $I = 0\,\mu\text{U}\,\text{ml}^{-1}$, $\beta = 0\,\text{mg}$) . The first and the third points have all their eigenvalues negative and hence are stable equilibrium points. The second point has two negative and one positive eigenvalue and hence is a saddle point. Topp, *et al.* referred the states associated with these points as physiological, unstable and pathological states respectively [24]. The solution comes either to a physiological or to pathological steady state depending on the initial condition for β. It was found that the

Table 3.1. Normal parameter values [24]

Parameter	Value	Units	Reference
S_I	0.72	$\mathrm{ml}\,\mu\mathrm{U}^{-1}\mathrm{d}^{-1}$	Finegood (1997)
E_{G0}	1.44	d^{-1}	Bergman *et al.* (1981)
			Finegood (1997)
R_0	864	$\mathrm{mg}\,\mathrm{dl}^{-1}\mathrm{d}^{-1}$	Bergman *et al.* (1981)
			Finegood (1997)
σ	43.2	$\mu\mathrm{U}\,\mathrm{ml}^{-1}\,\mathrm{d}^{-1}$	Bergman *et al.* (1981)
			Malaisse *et al.* (1967)
			Toffolo *et al.* (1980)
α	20000	$\mathrm{mg}^2\,\mathrm{dl}^{-2}$	Malaisse *et al.* (1967)
k	432	d^{-1}	Toffolo *et al.* (1980)
d_0	0.06	d^{-1}	Bergman *et al.* (1981)
			Imamura *et al.* (1988)
			Finegood *et al.* (1995)
r_1	0.84×10^{-3}	$\mathrm{mg}^{-1}\,\mathrm{dl}\,\mathrm{d}^{-1}$	Bergman *et al.* (1981)
			Imamura *et al.* (1988)
			Finegood *et al.* (1995)
r_2	0.24×10^{-5}	$\mathrm{mg}^{-2}\,\mathrm{dl}^2\,\mathrm{d}^{-1}$	Bergman *et al.* (1981)
			Imamura *et al.* (1988)
			Finegood *et al.* (1995)

global separatrix is perpendicular to the β-cell axis and passes through the saddle point [24]; that is, for initial values of β higher than 37 the system always comes to the physiological steady state, while for values less than 37 it always comes to pathological state.

3.2 Numerical results

In this section we present numerical results for the system (3.13). At both stable points there are significant spectral gaps between all eigenvalues, and hence one can use the ILDM method. Moreover, all the time scales can be separated, and hence the system (3.13) has both one- and two-dimensional slow manifolds. Both one- and two-dimensional manifolds were found using the ILDM method and plotted along with solutions for three special cases. Figures 3.1, 3.2, 3.3, 3.4, 3.5 and 3.6 show the solutions computed for those special cases as well as the projections of one dimensional ILDM on Glucose- β cell and Glucose-Insulin planes. On these plots the solutions are shown as bold lines. Figure (3.7) shows two dimensional ILDM, one dimensional ILDM, which is shown as a line of markers and few solutions of the system, which are shown as bold lines.

Figures (3.1) and (3.2) concern the effect studied by Bergman, *et al.* They found that increased plasma glucose, via an intravenous glucose injection, causes a rapid increase in plasma insulin followed by damped oscillations of both variables towards the preinjection steady state [3]. This observation is qualitatively consistent with Figure 3.1. The current model does not predict oscillations, which is an expected result, since the model was built under an assumption that fast insuline processes can be neglected. The way the system moves back to the equilibrium point becomes more clear if one looks at the three- dimensional Figure 3.7. After a very fast process of insulin increase the system comes to two-dimensional manifold and stays on it all the way back to the equilibrium point.

Figures 3.3 and 3.4 concern the effect of the β-cell mass reduction via administration of the β-cell toxin STZ on the system studied by Ferrand, *et al.* They found that the reduction generates transient hyperglycemia while the β-cell mass adapts [10]. This effect can be seen on figure 3.3. Figure (3.4) shows a quick fall in insulin

level caused by by decrease in insulin production rate due to reduction in β-cell mass. Again the three-dimensional Figure 3.7 shows that after a very quick fall in the insulin level the system comes on two dimensional manifold and stays on it all the way to one dimensional manifold where it stays until reaching the equilibrium point.

Figures 3.5 and 3.6 concern the case of the pathological solution. From figure 3.5 it can be seen that given low initial value of β, the system goes to the pathological hyperglycemia steady state even if an initial value of glucose is low. Here again, we have a very fast insulin process, which drives the system to the two-dimensional slow manifold where it goes until it reaches the one dimensional slow manifold where it stays all the way up to the pathological equilibrium point. This behavior is only partially consistent with the experimental data. Bernard, *et al.* showed that rats made hyperglycemic by STZ have β cells capable of increasing replication and decreasing death rates in response to glucose infusion; yet in the absense of glucose infusion, the rats remained hyperglycemic [4]. This implies that despite the prediction of the model there is no stable equilibrium point in the hyperglycemic region.

In summary, we can say that the model correctly describes some of the effects that are corroborated by the experiment; however, existence of two stable equilibria in the physiological region looks suspicious. We will return to this problem in the next section when analyzing the stability properties of the pathological fixed point. The other thing we would like to emphasize is a very fast insulin dynamics (on time scale of minutes) described by the model. This contradicts the initial assumption of slow dynamics, which were done when making a single-compartment approximation. Indeed, the model gives a good qualitative description of the glucose regulatory system.

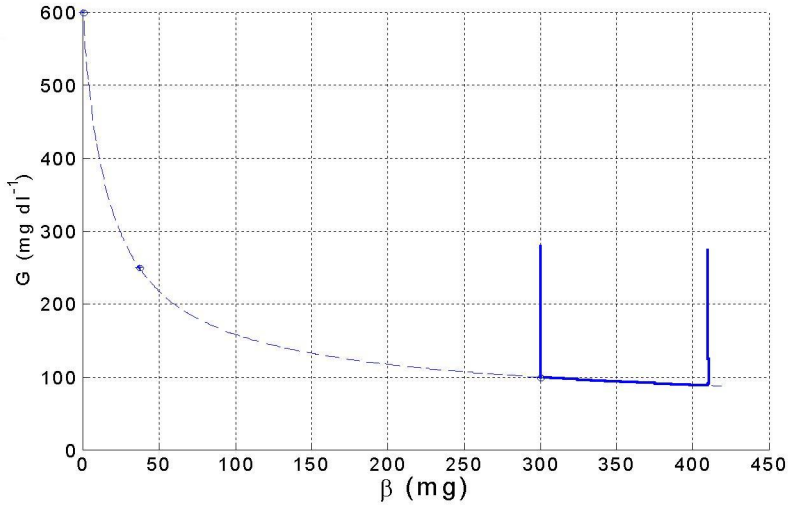

Figure 3.1. Glucose injection solution (G-β plane). One-dimensional ILDM is shown as a dashed line, solutions are shown as bold lines.

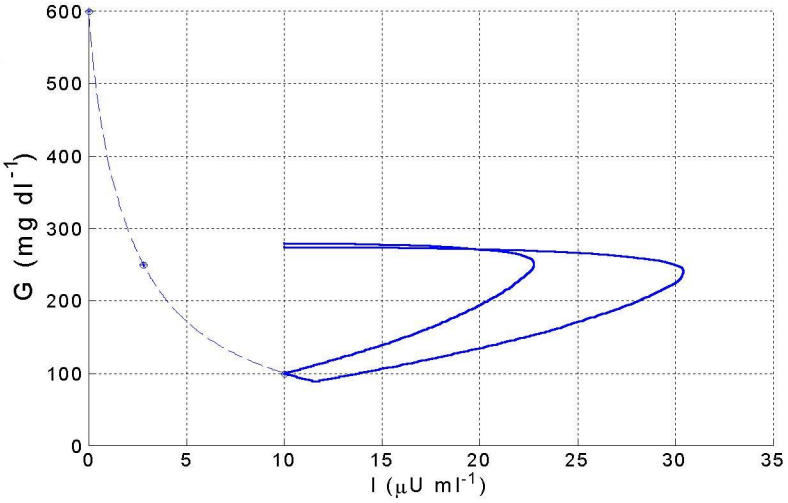

Figure 3.2. Glucose injection solution (G-I plane). One-dimensional ILDM is shown as a dashed line, solutions are shown as bold lines

.

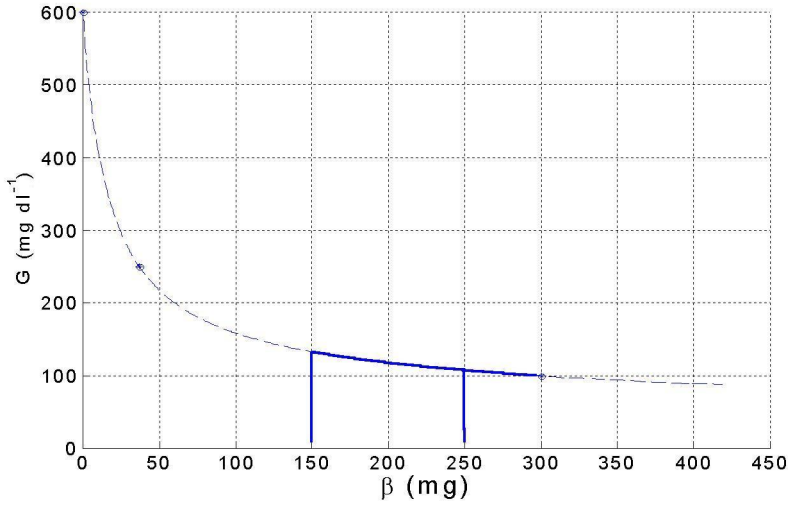

Figure 3.3. β-toxin injection solution (G-β plane). One-dimensional ILDM is shown as a dashed line, solutions are shown as bold lines.

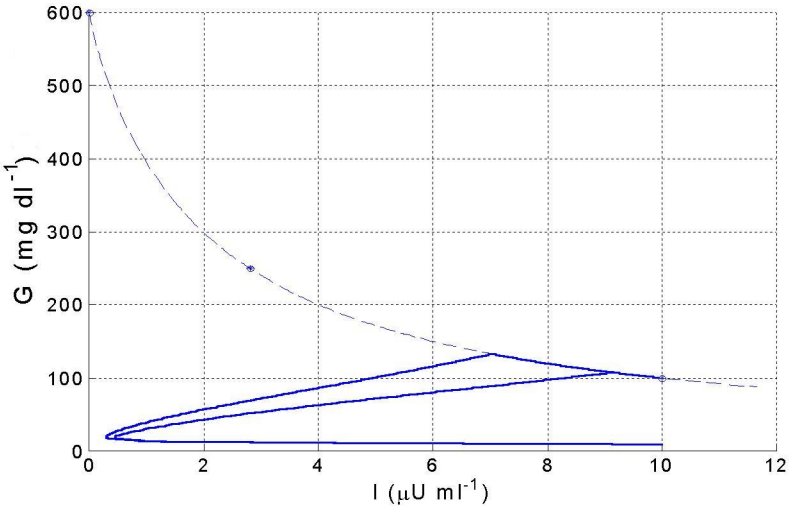

Figure 3.4. β-toxin injection solution (G-I plane). One-dimensional ILDM is shown as a dashed line, solutions are shown as bold lines.

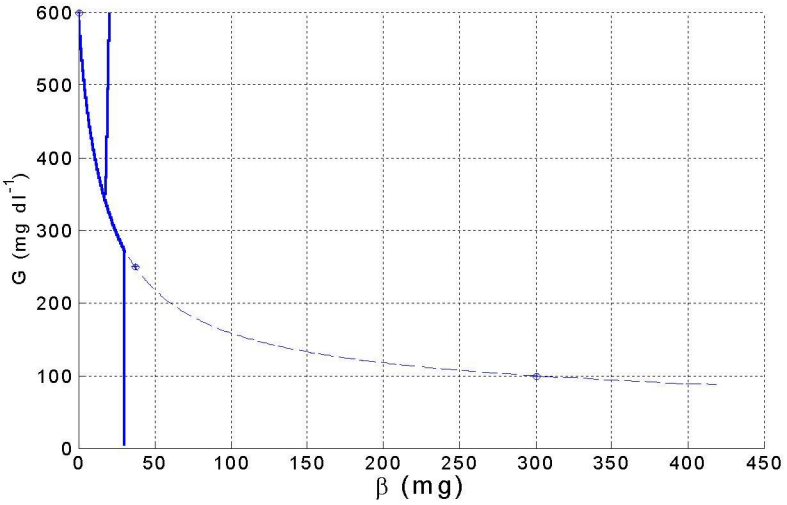

Figure 3.5. Pathological solution (G-β plane). One-dimensional ILDM is shown as a dashed line, solutions are shown as bold lines.

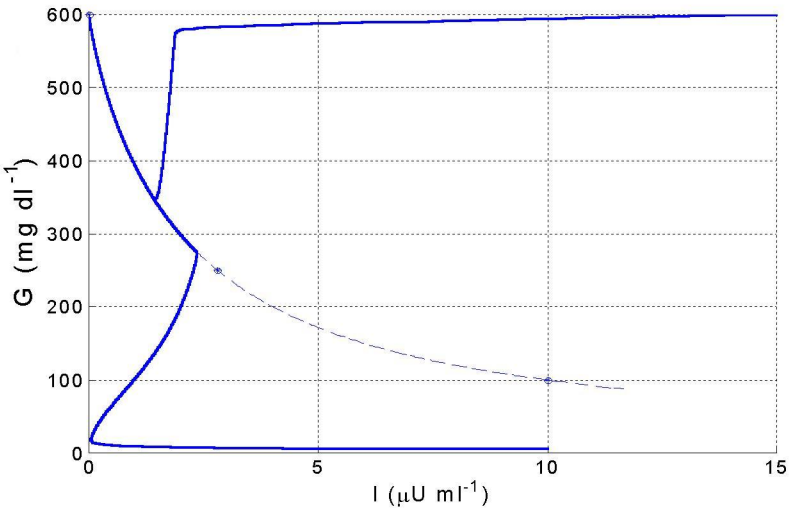

Figure 3.6. Pathological solution (G-I plane). One-dimensional ILDM is shown as a dashed line, solutions are shown as bold lines.

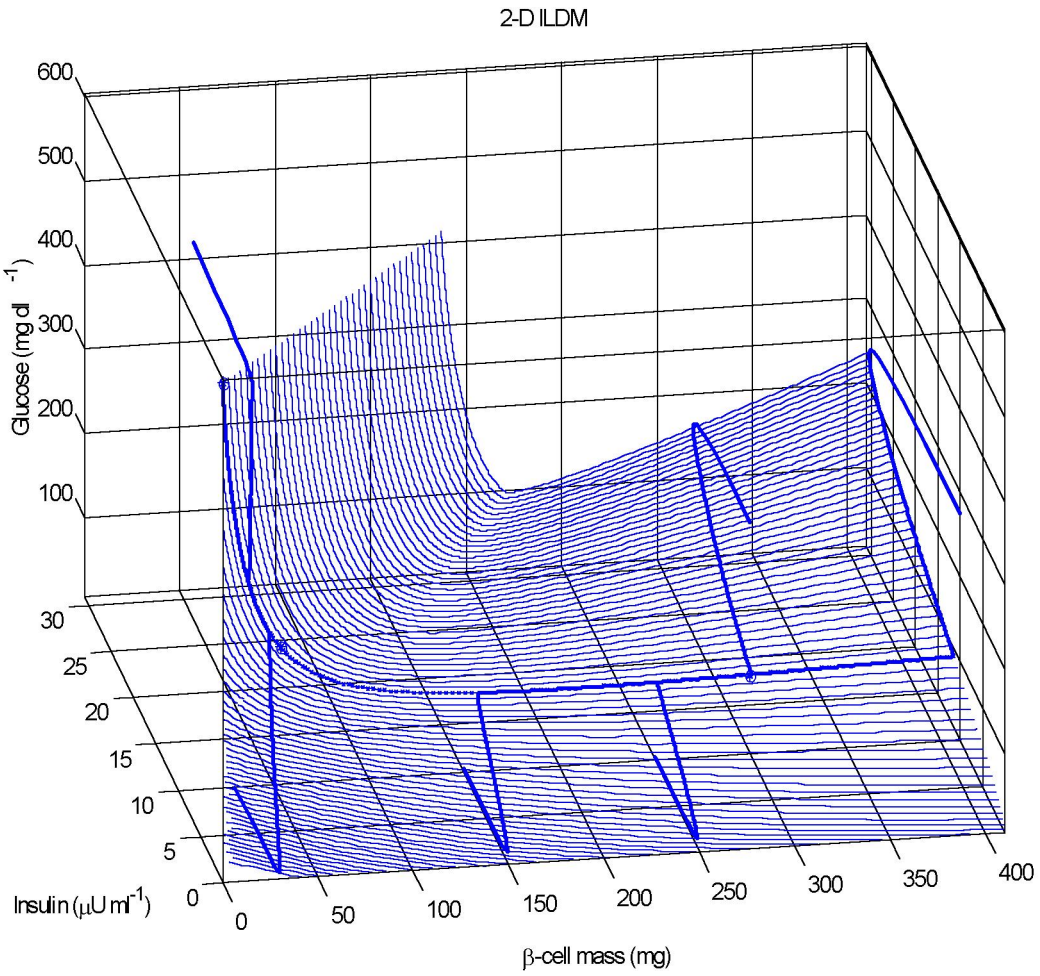

Figure 3.7. Three-dimensional picture (Two-dimensional ILDM, one-dimensional ILDM and solutions in special cases). Solutions are shown as bold lines.

3.3 Stability analysis and pathways to diabetes

In this section we perform stability analysis of the fixed points of the system (3.13) for different values of the parameters, study effects of parameter changes on behavior of the system, and consider special cases that give rise to diabetes.

3.3.1 Stability analysis

In general case the system (3.13) has three fixed points:

$$\begin{aligned} G_1 &= \frac{1}{2}\left(\frac{r_1}{r_2} - \sqrt{\left(\frac{r_1}{r_2}\right)^2 - 4\frac{d_0}{r_2}}\right) \\ I_1 &= \frac{R_0 - E_{G0}G_1}{S_I G_1} \\ \beta_1 &= \frac{kI_1(\alpha + G_1^2)}{\sigma G_1^2}, \end{aligned} \tag{3.14}$$

$$\begin{aligned} G_2 &= \frac{1}{2}\left(\frac{r_1}{r_2} + \sqrt{\left(\frac{r_1}{r_2}\right)^2 - 4\frac{d_0}{r_2}}\right) \\ I_2 &= \frac{R_0 - E_{G0}G_2}{S_I G_2} \\ \beta_2 &= \frac{kI_2(\alpha + G_2^2)}{\sigma G_2^2}, \end{aligned} \tag{3.15}$$

$$\begin{aligned} G_3 &= \frac{R_0}{E_{G0}} \\ I_3 &= 0 \\ \beta_3 &= 0, \end{aligned} \tag{3.16}$$

which for normal values of the parameters correspond to physiological, unstable and pathological steady states respectively.

First, we analyze the stability of the physiological steady point, assuming that it exists, that is:

$$\left(\frac{r_1}{r_2}\right)^2 - 4\frac{d_0}{r_2} > 0. \tag{3.17}$$

The eigenvalues of all three fixed points are the roots of the following equation:

$$\begin{vmatrix} -(E_{G0}+S_I I)-\lambda & -S_I G & 0 \\ \frac{2\alpha\sigma g\beta}{(\alpha+G^2)^2} & -k-\lambda & \frac{\sigma G^2}{\alpha+G^2} \\ (r_1-2r_2G)\beta & 0 & (-d_0+r_1G-r_2G^2)-\lambda \end{vmatrix} = 0. \tag{3.18}$$

For the physiological point we have:

$$-d_0+r_1G-r_2G^2=0, \tag{3.19}$$

and hence the equation (3.18) reduces to:

$$\begin{aligned} (-(E_{G0}+S_I I)-\lambda)(-k-\lambda)(-\lambda)- \\ (-S_I G)\left[\frac{2\alpha\sigma G\beta}{(\alpha+G^2)^2}(-\lambda)-\frac{\sigma G^2}{\alpha+G^2}(r_1-2r_2G)\beta\right] &= 0. \end{aligned} \tag{3.20}$$

After simplifications one obtains

$$\begin{aligned} \lambda^3+\lambda^2\left[k+(E_{G0}+S_I I)\right]+ \\ \lambda\left[k(E_{G0}+S_I I)+S_I\frac{2\alpha\sigma G\beta}{(\alpha+G^2)^2}\right]+ \\ S_I G\frac{2\alpha\sigma G\beta}{(\alpha+G^2)^2}(r_1-2r_2G)\beta &= 0. \end{aligned} \tag{3.21}$$

Now, we note that for the physiological fixed point:

$$G<\frac{1}{2}\frac{r_1}{r_2}, \tag{3.22}$$

and hence all the coefficients in the equation (3.21) are greater than zero. It immediately follows that the equation (3.21) has no positive roots, and therefore the physiological fixed point, if exists, is always stable. This fact is important for the consideration of the pathways to diabetes.

Next, we analyze the stability of the pathological fixed point. It exists for all the values of the parameters and has its eigenvalues defined by the following equation:

$$(E_{G0}+\lambda)(k+\lambda)\left[\lambda-(-d_0+r_1G-r_2G^2)\right]=0. \tag{3.23}$$

The equation (3.23) has two always negative roots and one either negative or positive root depending on the values of the parameters. Recalling that for the pathological fixed point

$$G = \frac{R_0}{E_{G0}}, \tag{3.24}$$

one can obtain:

$$\lambda_3 = -d_0 + r_1 \frac{R_0}{E_{G0}} - r_2 \left(\frac{R_0}{E_{G0}} \right)^2. \tag{3.25}$$

Therefore, stability of the pathological fixed point depends on parameters determining glucose dynamics as well as the parameters determining β-cell dynamics. In terms of the current model, the normal values of the parameters give rise to a negative λ_3 and hence to a stable pathological point. However, we expect that more precise model of β-cells dynamics may change this situation, so that there will be only one stable fixed point (either physiological or pathological, depending on the values of the parameters) in the physiological region.

3.3.2 Pathways to diabetes

Analysis in the previous subsection showed that the physiological fixed point, if exists, is always stable; therefore, one obvious pathway to diabetes is the change in the parameters of the system that eliminates the physiological and the saddle fixed points. It occurs when

$$\left(\frac{r_1}{r_2} \right)^2 - 4 \frac{d_0}{r_2} < 0. \tag{3.26}$$

Equation (3.26) is solely determined by the parameters of the β-cell dynamics, and hence this pathway results from defects in β-cell mass dynamics. In terms of current model, this situation takes place when the death rates exceed the replication rates for all values of glucose. It leaves only pathological point with zero β-mass and insulin. This pathway was referred by Topp, *et al.* as a bifurcation pathway [24]. It resembles type 1 diabetes mellitus (insulin dependent diabetes). An autoimmune

attack on the pancreatic β-cells increases death rates above the replication rates, and the β-cell mass falls towards zero [18].

The other possible pathway contained in the model takes place when a change in the parameters shifts the physiological fixed point towards the hyperglycemic level, causing persistent hyperglycemia. The equation (3.14) shows that it can result from changes in the parameters of the β-cell dynamics. The other way implicitly contained in the model is to couple a loss of β-cell mass regulation to deffects in glucose and/or insulin dynamics. Setting each of the β-cell mass parameters to zero yields equal replication and death rates at all glucose levels, and hence the β-cell mass becomes nonresponsive. In that case the model reduces to just two equations, and defects in any of the glucose or insulin parameters can generate hyperglycemia. Topp, *et al.* proposed that this pathway may fit the human autopsy data. Pancreas from obese nondiabetic subjects have a larger than normal β-cell mass, while obese people with diabetes have normal β-cell mass levels. In the later subjects, a coupling of insulin resistance due to obesity, to a non-adaptive β-cell mass may be a cause of their diabetes. If this idea is correct, than this pathway fits type 2 diabetes mellitus (non-insulin dependent diabetes).

CHAPTER 4

SUMMARY AND DISCUSSION

In this thesis two major topics have been considered: theoretical development of the ILDM method and dynamics of the glucose regulatory system. Here we give a brief summary of the results obtained and outline the directions for future research.

In the ILDM section, the justification of the method was given. A general case of the nonlinear dynamical system with a stable sink type equilibrium point was considered. The only assumption made about the system was the assumption of a significant gap in the eigenvalue spectrum computed at the equilibrium point. It was shown that under the assumption made, the system reduces to a singular perturbation problem with a small parameter equal to the quantity inverse to the wideness of the gap. It was shown that Maas-Pope formula gives a first approximation of the solution with respect to the small parameter. The derivation was consequently done for the linear systems, when the formula is exact in the sense explained, nonlinear system with the only spectral gap, and finally for the general case of a nonlinear system with any number of spectral gaps. In the nonlinear case the formula was rigorously proved for a small vicinity of the equilibrium point, extending the formula required an additional assumption about the behavior of the eigenvalues far from the equilibrium point. Such an assumption cannot be checked directly, which designates the first direction of future research. This problem is that of linear algebra, and the point here is to find a way to make an estimate of the eigenvalues far from the equilibrium point based only on the Jacobian matrix. The other direction comes

from the fact that the spectral gap gives only a sufficient condition for existence of the slow manifold, and so it would be interesting to find out if it is a necessary condition as well.

In the part concerned with the glucose regulatory system a coupled glucose-insulin-β-cells model introduced by Topp, *et al.* [24] was considered. Using the ILDM method helped to better understand the dynamics of the system when it was compared with experimentally established effects. Ability to obtain a two dimensional ILDM was especially helpful in those considerations. Stability analysis was also useful and confirmed some of the results presented without proof in the original work done by Topp, *et al.* It was found that if the physiological steady state exists it is always stable. This fact, supports the conclusion made by Topp, *et al.* that the model (if no additional complications are done) has two possible pathways to diabetes. The bifurcation pathway occurs when defects in β-cell mass dynamics drive death rate of the β-cells higher than the replication rate for all level of glucose and the physiological and the saddle state states stop to exist. This pathway corresponds to the first type of diabetes. The other pathway supposedly corresponds to the second type of diabetes. It is caused by shifting the physiological point towards hyperglycemic levels. It can be caused either by defects in β-cell mass dynamics or by making β-cell mass nonresponsive to the changes in glucose level, that is by decoupling the β-cell dynamics from the model, in addition to an abnormality in glucose and or insulin dynamics.

The weakest point in the model is the presence of two stable equilibrium points simultaneously. The stability analysis of the pathological steady point showed that this situation may be changed if β-cell dynamics is modeled more thoroughly. For example, incorporating into the model additional processes such as neogenesis can make the pathological point unstable for the range of the parameters for which

physiological steady point exists. We see this as a possible direction for future research.

The other weak point in the model is fast insulin processes which were found to take place. This contradicts the basic assumption of the slow dynamics that were made to justify the single-compartment approximation. We see building multicompartment models as a very intresting direction for future research.

BIBLIOGRAPHY

[1] J. R. Allsop, R. R. Wolfe, J. F. Burke. The reliability of rates of glucose appearance *in vivo* calculated from constant tracer infusions. *Biochemestry Journal*, 172:407-416, 1978.

[2] R. N. Bergman, D. T. Finegood, M. Ader. Assesment of insulin sensitivity *in vivo*. *Endocrine Reviews*, 6:45-58, 1985.

[3] R. N. Bergman, Y. Z. Ider, C. R. Bowden, C. Cobelli. Quantitative estimation of insulin sensitivity. *American Journal of Physiology*, 236:E667-E677, 1979.

[4] C. Bernard, M. F. Berthault, C. Saulnier, A. Ktorza. Neogenesis vs. apoptosis as main components of pancreatic beta-cell mass changes in glucose-infused normal and mildly diabetic adult rats. *FASEB Journal*, 13:1195-1205, 1999

[5] C. Cobelli, G. Pacini. Insulin secretion and hepatic extraction in humans by minimal modeling of C-peptide and insulin kinetics. *Diabetes*, 37:223-231, 1988.

[6] C. Cobelli, G. Pacini, A. Salvan. On a simple model of insulin secretion. *Journal of Medical and Biological Engineering and Computing.*, 18:457-463, 1980

[7] M. J. Davis, R. T. Skodje. Geometric investigation of low-dimensional manifolds in systems approaching equilibrium. *Journal of Chemical Physics*, 111:859-874, 1999.

[8] P. Deuflhard, B. Fiedler, P. Kunkel. University of Heidelberg, SFB 1233, Technical Report 278, 1984

[9] I. B. Efanova , S. V. Zaitsev, B. Zhivotovsky, M. Kohler, S. Efendic, S. Orrenius, P. O. Berggren. Glucose and tolbutamide induce apostosis in pancreatic β-cells. *Journal of Biological Chemestry*, 273:33501-33507, 1998.

[10] N. Ferrand, A. Astesano, H. H. Phan, C. Lelong, G. Rosselin. Dynamics of pancreatic cell growth and differentiation during diabetes reversation in STZ treated new born rats. *American Journal of Physiology*, 269:C1250-C1265, 1995.

[11] D. T. Finegood, L. Scaglia, S. Bonner-Weir. Dynamics of β-cell mass in the growing rat pancreas estimation with a simple mathematical model. *Diabetes*, 44:249-256, 1995.

[12] S. J. Fraser. The steady state and equilibrium approximations: A geometric picture. *Journal of Chemical Physics*, 88:4732-4738, 1988.

[13] S. R. Hugl, M. F. White, C. J. Rhodes. Insulin-like growth factor I (IGF-I)-stimulated pancreatic β-cell growth is glucose dependent. *Journal of Biological Chemestry*, 273:17771-17779, 1988.

[14] G. Kloppel, M. Lohr, K. Habich, M. Oberholzer, P. U. Heitz. Islet pathology and the pathogenesis of type 1 and type 2 diabetes mellitus revisited. *Surveys in Synth Pathology Research*, 4:110-125, 1985.

[15] U. Maas and S. B. Pope. Simplifying chemical kinetics: Intrinsic low-dimensional manifolds in composition space. *Combustion Flame*, 88:239-264, 1992.

[16] W. Malaisse, F. Malaisse-Lagae, P. H. Wright. A new method for the measurement *in vitro* of pancreatic insulin secretion. *Endocrinology*, 80:99-108, 1967.

[17] H. Neimann, D. Schmidt, U. Maas. An efficient storage scheme for reduced chemical kinetics based on orthogonal polynomials. *Journal of Engineering Mathematics*, 31:131-142, 1997

[18] B. A. O'Brien, B. V. Harmon, D. P. Cameron, D. J. Allan. Beta-cell apoptosis is responsible for the development of IDDM in the multiple low-dose streptozotocin model. *Journal of Pathology*, 178:176-181, 1996.

[19] C. Rhodes, M. Morari, S. Wiggins. Identification of low order manifolds: Validating the algorithm of Maas and Pope. *Chaos*, 9(1):108-123, 1999.

[20] M. R. Roussel, S. J. Fraser. Invariant manifold methods for metabolic model reductions. *Chaos*, 11:196-206, 2001.

[21] D. Schmidt, T. Blasenberg, U. Maas. Intrinsic low-dimensional manifolds of strained and unstrained flames. *Combustion Theory and Modeling*, 2:135-152, 1998.

[22] S. Singh, J. M. Powers, S. Paolucci. On slow manifolds of chemically reactive systems. *Journal of Chemical Physics*, 117:1482-1496, 2002

[23] G. Toffolo, R. N. Bergman, D. T. Finegood. C. R. Bowden, C. Cobelli, Quantitative estimation of β-cell sensitivity to glucose in the intact organism: a minimal model of insulin kinetics in the dog. *Diabetes*, 29:979-990, 1980.

[24] B. Topp, K. Promislow, G. deVries, R. Miura, D. Finegood. *Journal of Theoretical Biology*, 206:605-619, 2000.

[25] B. Yang and S. B. Pope. An investigation of the accuracy of manifold methods and splitting schemes in the computational implementation of combustion chemistry. *Combustion and Flame*, 112(1-2):16-32, 1998.